International Journal of Maritime Engineering

THE HYDRODYNAMIC AND DYNAMIC MOTION ANALYSIS OF A DAMAGED SHIP

G E Hearn, University of Southampton, UK
D Lafforgue and **E Perdriset,** Ecole Nationale Supérieure d'Arts et Métiers (ENSAM)
D Saydan, Bureau Veritas, Turkey

SUMMARY

The hydrodynamic analysis and motion response of a damaged ship requires a novel generalisation of the methods normally applied to intact ships or other floating structures. Damaged ship statistics are used to provide likely damage scenarios. Water ingress, arising from the hull damage will require special attention regarding the influence of the presence of internal free surfaces and the modelling of the air stiffness associated with the within cargo hold air located between the internal movable free surface and the deck. The additional ideas required are developed and applied to a damaged optimised bulk carrier, the Derbyshire. This hull form is selected because of the well-publicised available associated structural details.

NOMENCLATURE

A, B, C & D	Different damage scenarios as defined in Table 1
$A, \delta A, A^{-1}$	Hydrodynamic influence matrix, its associated numerical error and inverse respectively
AP, FP	Aft / forward perpendicular
A_o or $A_o^{FS_i}$	Cross sectional area of general or specifically selected internal free surface
A_{kj}, B_{kj}	Reactive coefficients of added mass and fluid damping for k^{th} direction force (moment) due to motion in j^{th} direction for the case of a single body fluid-structure interaction problem
$A_{kj}^{S_A S_B}, B_{kj}^{S_A S_B}$	Generalised added mass and fluid damping reactive coefficients associated with hydrodynamic force / moment acting on structure S_A in k^{th} direction as a consequence of structure S_B moving in j^{th} degree of freedom
$A_{S_A}^{S_B}$	Hydrodynamic influence sub-matrix indicating influence of structure S_B on structure S_A
a	Amplitude of progressive harmonic and regular incident wave
B	Breadth (or moulded) beam of ship
b	Penetration depth of ship damage
$b, \delta b$	Hydrodynamic wetted surface boundary condition related influence vector and associated numerical error
b^{S_A}	Subdivision of vector b related to structure S_A
C_{kj} or $C_{kj}^{S_A S_A}$	Hydrostatic restoration force (moment) coefficient in k^{th} direction on structure S_A as a consequence of the j^{th} degree of freedom being invoked on structure S_A
D	Depth of intact ship
DS, IS	Damaged ship and intact ship respectively
dS	Elemental wetted surface area associated with integration of different forces
F	General hydrostatic force introduced in Section 2.4
FS_i	Internal free surface of water within i^{th} hold
$F_k^{S_A}$	Excitation wave load in k^{th} direction on structure S_A
$F_k^{S_A\ Direct}$	$F_k^{S_A}$ evaluated directly using the incident and the diffraction velocity potentials ϕ_I and ϕ_D respectively
$F_k^{S_A\ Haskind}$	$F_k^{S_A}$ evaluated using the Haskind relationship and the incident and the radiation velocity potentials ϕ_I and ϕ^k respectively
F_{kj} or $F_{kj}^{S_A S_B}$	Reactive force (moment) in k^{th} direction due to same structure moving in j^{th} direction or reactive force (moment) on structure S_A in k^{th} direction due to structure S_B moving in j^{th} direction
g	Gravitational acceleration
h	Height (not vertical position) of ship damage

Im, Re	Subscripts denoting imaginary and real parts of complex quantity
I_{44}, I_{55}, I_{66}	Moments of inertia associated with roll, pitch and yaw
I_{45}, I_{46}, I_{56}	Products of inertia required for damaged ship with $I_{jk} = I_{kj}$
i	Pure imaginary number, general subscript or subscript identifying a particular internal free surface
$K(A)$	Conditioning number of matrix A
K_{air}, K_{air}^{T}	Isentropic and isothermal air stiffness in hold as a consequence of volume change
K_{air}^{+}, K_{air}^{-}	Equivalent spring isentropic air stiffness model for positive (0 to y_{peak}) and negative (- y_{peak} to 0) moments of internal free surface
k, j	Subscripts denoting force (moment) direction and motion degree of freedom respectively
L	Ship length scale
L_h	Horizontal extent of ship damage
l_i	Pitch lever measured from reference system origin to static equilibrium position of the centroid of the i^{th} internal free surface of damaged ship
M	Ship total mass consistent with intact or damaged scenario being addressed
N	Total number of boundary elements used to model specific fluid structure interaction
n	Direction normal to fluid or structural boundary surface
n_k or $n_k^{S_A}$	Generalised direction cosine associated with k^{th} direction of general structure or specific structure S_A
P, V	Pressure and volume associated with air within cargo hold
P_o, V_o	Ambient representative atmospheric pressure and associated volume in selected hold at this pressure
P_{eq} or $P_{eq}^{FS_i}$	Equilibrium pressure within i^{th} hold taking into account motion of damaged ship
RVM or $RVM_{FS_i}^{DS}$	Magnitude of resultant vertical motion of ship at selected point or of damaged ship (DS) at point coincident with mean position of centroid of i^{th} internal free surface (FS_i)
S_A, S_B	Superscripts denoting distinct structures or substructures
$S_W^{S_A}$	Integration domain based on 'wetted' surface of structure or substructure S_A
$\ddot{s}_j^{S_A}, \dot{s}_j^{S_A}, s_j^{S_A}$	Denote acceleration, velocity and displacement of structure or substructure S_A in the j^{th} degree of freedom. Absence of superscript S_A denotes one structure only being investigated
$s_{ja}^{S_B}$	Magnitude of motion in the j^{th} degree of freedom on structure S_B used in specification of radiation wetted surface boundary condition specification. May be set to unity without loss of generality
T	As a superscript indicates either matrix transposition or isothermal value of air stiffness
T_n	The n^{th} term of a series
t	Time
X_{CG}, Y_{CG}, Z_{CG}	Coordinates of centre of gravity of ship
X_{FS}, Y_{FS}, Z_{FS}	Coordinates of centroid of an internal free surface (FS)
x, y, z	Cartesian righted handed coordinate system with x-axis positive to port, y-axis positive above undisturbed external free surface and z-axis positive towards the bow
Y	Vertical location of ship damage or used to indicate a particular value of coordinate y
y_{eq} or $y_{eq}^{FS_i}$	Air gap associated with equilibrium pressure when motion of ship taken into account
y_{peak} or $y_{peak}^{FS_i}$	Magnitude of resultant vertical motion of selected internal free surface
y_o or $y_o^{FS_i}$	Mean air gap between selected internal free surface and deck
y_1, y_1^{T}	Isentropic and isothermal mean position of internal free surface as a consequence of ship motion
α	Solid angle subtended at centroid of boundary element
β	Wave heading defined with respect to positive forward z-axis, 180^o corresponds to a head sea
γ	Ratio of specific heat capacities at constant pressure and constant volume
Δ	Change in physical quantity it precedes, e.g. ΔF denotes force change
ρ	Fluid density

Φ^j, Φ_D, Φ_I	Time dependent velocity potential for radiation problem for j^{th} degree of freedom, for diffraction problem and known incident velocity potential respectively
$\phi, \delta\phi$	Sought time independent velocity potential and associated numerical error
ϕ^{S_A}	Subdivision of sought velocity potential vector ϕ related to structure S_A
ψ	Kernel of Fredholm integral equation corresponding to velocity potential for 3D pulsating source
ω	Circular frequency (rad./s) associated with incident wave or ship responses
$\|Q\|$	Euclidean norm of quantity Q

1. INTRODUCTION

Earlier reported research [Day and Doctors (1997), Doctors & Day (1995), Hearn et al (1992, Hearn et al (1995a, 1995b), Hearn & Wright (1998,1999), Sarıoz et al (1992), Sarıoz (1997) et cetera] has investigated the simultaneous optimisation of the seakeeping and resistance characteristics (frictional, wave making and added) of very different monohull forms (warships, fishing boats, containerships) and catamaran forms. For monohulls the well-known Hooke & Jeeves [1961] optimisation procedure is more than adequate, but for catamarans a Genetic Algorithm approach [Hearn & Wright (1998,1999), Wright (2004)] was adopted to seek out a global optimum from numerous localised optimum. The optimisation in each case was achieved subject to satisfaction of the usual IMO intact stability requirements.

The success of the research, the ability to improve seakeeping responses and the overall resistance with intact stability, whilst pleasing, subsequently forced the principal author to put the question: 'If the seakeeping and resistance characteristics are both improved without intact stability being compromised, where do the penalties lie?' Surely it would be extremely perverse if the damaged optimised ship exhibited motion responses significantly larger than the damaged original design. More recent research undertaken by Saydan & Hearn (2004) and Saydan (2006) has addressed this question. However, to damage either the original design or the optimised design requires some insight regarding the cause and most likely outcomes of damage for the selected ship type. Using statistics [Saydan (2006)] derived from damaged ship databases, covering the periods 1935 to 1999 and 1992 to 2002, a bulk carrier hull form (based on Derbyshire) was optimised and then the parent and optimised hull forms were damaged with location, extent and depth of damage applied according to the most likely scenarios the analysed damage statistics suggested. The damage statistics applied resulted in water ingress into the damaged hold(s).

The water ingress naturally leads to changes in heel and trim and this necessitated the development of a novel method to estimate the products of inertia of a damaged ship [Saydan & Hearn (2004) and Saydan (2006)], in order to undertake meaningful comparisons of the intact and the damaged ship motion responses. Even if one makes the usual assumption of neglecting the products of inertias for the intact ship, as soon as the ship heels or trims it loses the implicitly assumed mass distribution symmetry and hence the products of inertia will be non-zero. Heel and trim together will remove the geometric (port starboard) symmetry of the intact ship form.

In earlier analyses new static equilibrium positions for the damaged parent and optimised hull forms, as a consequence of water ingress, preceded the hydrodynamic and dynamic motions of the parent and optimised intact and damaged hull forms. The damage naturally modifies the hydrostatic restoration terms, the hydrodynamic radiation and wave excitation loading terms and the associated mass- inertia matrix. Apart from these influences the existence of the internal free surfaces was not explicitly included in the original hydrodynamic analyses, Saydan (2006). The subsequent motion analysis suggested that the relative vertical motions of the damaged optimised hull form could be more significant than the damaged parent hull in some situations.

The quality of the proffered possible conclusion must, in part, rest with the extent and quality of the details related to the modelling of the selected damage scenarios, the related hydrodynamic modelling and motion analysis executed. Therefore in this paper the work of Saydan (2006) has been significantly extended to investigate explicitly the influences of the internal free surfaces, with their assumed rigid body degrees of freedom, and the aerostatic influences of the in-hold air above the internal free surfaces. For completeness a minor investigation of non-linear viscous roll damping is included.

The selected damage scenarios for the Derbyshire, based on the cited damage statistic databases, are defined in Section 2. The remainder of Section 2 indicates how the hydrodynamic modelling was performed and provides standard fluid structure interaction related concepts together with necessary generalisations of the added mass and fluid damping definitions required to facilitate the multi-body approach of the subsequent generalised motion response analysis. This generalisation requires development of stiffness expressions for the in-hold air. The choices regarding the modelling of the internal air stiffness are developed from first principles in Section 3. The new generalised dynamic motion response equations and the method of solution is provided in Section 4 with representative results presented and discussed in Section 5. The paper closes with the principal conclusions and

an indication of the obvious application of the proposed analysis to other fluid structure interaction analyses.

The analysis of the Derbyshire is undertaken because of the amount of public domain information available concerning the hull form geometry and mass distribution. This is a prerequisite to the analysis performed. It is not the intention of this paper to suggest that the analysis presented would or could assist with the provision of an explanation for the sad loss of the Derbyshire.

2. THE DAMAGED HULL

The original analysis considered four distinct damage scenarios designated A, B, C & D for parent hull and hull optimised for vertical relative bow motion [Saydan (2006)]. In each case the damage was sustained below the waterline on the starboard side of the ship. The vertical location of the damage relative to the hull form base line, Y/D, together with the horizontal extent, L_h/L, the damage height, h/D, and the depth of the damage, b/B, was determined from a statistical analysis of the damage databases for bulk carriers. The statistics indicated that the most likely longitudinal position of the damage would be in the region defined by the forward perpendicular (FP) and the station $L/4$ aft of FP. The horizontal extent of the damage L_h was unlikely to exceed $0.06L$. Hence these two constraints imply that damage may: (i) occur within any particular hold within the defined region, (ii) occur in any pair of holds if damage located near a bulkhead separating adjacent holds and (iii) can not affect 3 cargo holds simultaneously. Table 1, involving Cargo Holds 1 to 3 illustrated in Figure 1, indicates the different individual and paired cargo holds damaged and the associated values of defined parameters.

Table 1. Damage scenarios for optimised Derbyshire hull form

Scenario	Y/D	L_h/L	h/D	b/B	**Hold**
A	0.2	0.02	0.2	0.2	2
B	0.2	0.06	0.2	0.2	2
C	0.2	0.06	0.4	0.2	1 & 2
D	0.2	0.06	0.4	0.2	2 & 3

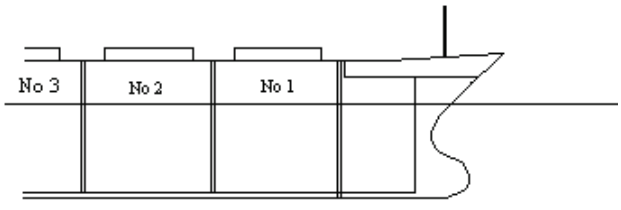

Figure 1 – The designation of damaged cargo holds referenced in Table 1

The amount of parallel sinkage, heel and trim arising as a consequence of application of the damage scenarios is provided in Table 2.

In this paper only scenarios A and C are to be revisited. They represent the smallest set and largest set of combined heel & trim angles irrespective of considering damaged parent hull form or damaged optimised hull form.

Table 2. Hull orientation changes resulting from application of damage scenarios

Damaged Parent Hull Attitude	Scenario A	Scenario B	Scenario C	Scenario D
Parallel Sinkage (m)	1.037	1.243	1.992	2.035
Trim Angle (^{o})	0.964	1.192	1.875	1.470
Heel Angle (^{o})	1.224	1.287	2.000	2.000

With the damage scenarios defined the hydrodynamic analysis requirements is developed next.

2.1 HYDRODYNAMIC MODELLING OF INTACT AND DAMAGED SHIP

The fluid is assumed to be inviscid and incompressible, and subject to irrotational flow. The three dimensional (3D) partial differential equation (PDE) description of the radiation and diffraction fluid-structure interactions [Faltinsen & Michelsen (1974), Hogben & Standing (1974), Odabasi & Hearn (1977)] includes: linearization of the composite free surface boundary condition, expressing continuity of fluid pressure and fluid velocity across the free surface; linearization of the wetted surface normal velocity boundary condition; an appropriate Sommerfeld radiation condition applied at large horizontal distances from the fluid structure interaction investigated. The seabed is assumed flat, horizontal and impermeable.

The conversion of the partial differential equation formulation of the fluid–structure interaction analysis to a Fredholm second-kind integral equation formulation is readily achieved using Green identities. The mathematical details of this conversion readily indicate that the wetted surface, defining the domain of the associated Fredholm integral, is not required to be continuous per se. Hence generalisation of its application to multi-bodied or segmented /articulated structures simply requires management of such options within the software, rather than a generalisation of the single body based mathematical analysis.

The hydrodynamic modelling of rigid or articulated floating structures, fixed structures or a mixture of

structural types of arbitrary geometric form can thus be readily modelled and analysed using boundary element formulations of the indicated fluid-structure interactions. The boundary element formulation applied here uses a second-kind Fredholm integral equation (FIE) formulation to determine directly the required radiation and diffraction velocity potentials.

Since the damaged ship hull scenarios will (as indicated previously) lead to water ingress the fluid-structure interaction must model, in addition to the normal six rigid degrees of freedom of a floating structure, those degrees of freedom attributed to each distinct internal free surface. The hydrodynamic interactions of the ship and the free surface(s) will be modelled by defining appropriate combinations of boundary conditions on the wetted surface of the ship and the distinct internal free surface(s). In particular, the ship degrees of freedom will be invoked one at a time, in turn, subject to the internal free surface(s) remaining fixed, whereas the heave, roll and pitch degrees of freedom of a free surface will be invoked, one at a time, in turn, with the damage ship and any other internal free surface present assumed stationary.

This approach permits provision of the required cause and effect hydrodynamic loads necessary to formulate the coupled equations of motion for the total number of degrees invoked; six for an intact ship, nine for a damaged ship with one internal free surface (Scenario A) and twelve degrees of freedom for a damaged ship with two internal free surfaces (Scenario C). Obviously, as indicated in Table 2, the intact and damaged ships assume different attitudes (orientations) in their static equilibrium states and hence exhibit different hydrodynamic loads when incident waves are introduced or the structures are force oscillated in the selected degrees of freedom. The modelling of the coupled motions of the internal free surface(s) and the damaged ship motions is addressed in some detail in Section 3.

The sizing, positioning and orientation of the boundary elements over the wetted surface must provide geometric characteristics consistent with the actual wetted surface area of the underwater portion of hull, the volume of the displaced fluid, as well as provide representative distributions of the wetted surface body conditions for all radiation and diffraction fluid-structure interaction problems investigated, for each of the wave frequencies and wave headings considered.

Table 3 indicates the number and shape of the boundary elements used in the hydrodynamic analyses of the optimised Derbyshire hull form and Figure 2 provides discretised hull form and internal free surfaces for scenario C.

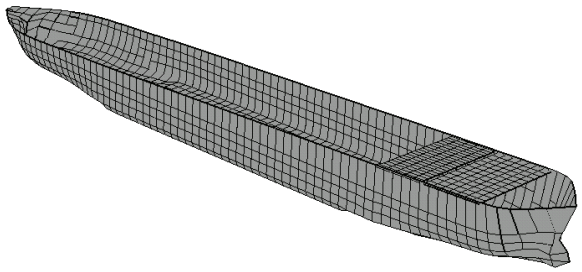

Figure 2 - Discretised damaged optimised Derbyshire hull form and internal forward free surfaces of scenario C

Objective assessment of the quality of the velocity potential solutions provided, and the hydrodynamic loadings discussed next, will be addressed in Section 2.3

2.2 PREDICTION OF RADIATION AND DIFFRACTION FLUID LOADINGS ON INTACT SHIP

Throughout the paper zero forward speed will be assumed since any rescue or assessment scenario would initially occur under these conditions. The intact ship will be modelled with the usual six degrees of freedom. Having invoked in turn each degree of freedom, for each circular frequency value ω, the resulting radiation forces and moments acting in the k^{th} direction due to the ship moving in j^{th} direction is expressed as

$$F_{kj}(\omega) = -A_{kj}(\omega)\ddot{s}_j(\omega) - B_{kj}(\omega)\dot{s}_j(\omega) \quad : k, j = 1, 2, \ldots, 6. \tag{1a}$$

Table 3. Discretisation levels for completed hydrodynamic analysis

Element Type → Ship Status ↓	**Quadrilateral Elements**	**Triangular Elements**	**Total Number of Boundary Elements**
Intact	1294	20	1314
Damage Scenario A	1294	20	1314
Damage Scenario A + FS2	1294 100	20	1414
Damage Scenario C	1285	22	1307
Damage Scenario C + FS2 + FS1	1285 100 84	22	1491

Here $A_{kj}(\omega)$ and $B_{kj}(\omega)$ denote the hydrodynamic added mass / inertia and fluid damping coefficients. Writing the radiation velocity potential as

$$\Phi^j(x,y,z;t) = [\phi^j_{Re}(x,y,z) + i\,\phi^j_{Im}(x,y,z)]\exp(-i\,\omega\,t),$$

with ω denoting the circular frequency of oscillation, it is readily shown that

$$A_{kj}(\omega) = \frac{\rho}{\omega s_{ja}}\iint_{S_W}\phi^j_{Im}\,n_k\,dS = \frac{\rho}{\omega s_{ka}}\iint_{S_W}\phi^k_{Im}\,n_j\,dS = A_{jk}(\omega)$$

and (1b)

$$B_{kj}(\omega) = \frac{-\rho}{s_{ja}}\iint_{S_W}\phi^j_{Re}\,n_k\,dS = \frac{-\rho}{s_{ka}}\iint_{S_W}\phi^k_{Re}\,n_j\,dS = B_{jk}(\omega).$$

The domain of integration is the wetted surface of the structure. The wave excitation forces and moments are a consequence of the scattering of the incident wave by the structure. This is investigated for each incident wave frequency (equal to each radiation frequency considered) for each wave heading of interest, β. In general the incident wave potential is written as

$$\Phi_I(x,y,z,t) = \alpha\frac{ag}{\omega}\frac{\cosh[k(y+d)]}{\cosh(kd)}\exp(i[k(z\cos\beta + x\sin\beta) - \omega t]) \quad (2a)$$

with z positive forward, x positive to port and y positive upwards from the undisturbed free surface. Hence a head sea corresponds to $\beta = 180^o$. The resulting wave excitation in the k^{th} direction is thus

$$F_k(\omega,\beta) = -i\omega\iint_{S_W}[\phi_I + \phi_D]\,n_k\,dS\exp(-i\,\omega\,t) : k = 1,2,..,6. \quad (2b)$$

In the so-called 'straightforward' motion analysis of the Derbyshire, Equations (1b) & (2b) will be used in Section 2.5 whether the Derbyshire is assumed to be intact or damaged. In either case the appropriate definition of S_W will be applied. The loadings of Equations (1b) & (2b) are determined using the MATTHEW diffraction suite of computer programs.

2.3 GENERALISED RADIATION AND DIFFRACTION FLUID LOADINGS ON A DAMAGED SHIP

For the damaged ship the total wetted surface can be deemed to be the union of the wetted surface of the damaged ship and the internal free surfaces resulting from the ingress of water into the damaged hold(s). That is, we may write $S_W = S_{DS} \bigcup S_{FS_2}$ for damage scenario A and $S_W = S_{DS} \bigcup S_{FS_2} \bigcup S_{FS_1}$ for damage scenario C of Table 1. Clearly DS, FS_1 and FS_2 denote the damaged ship's wetted surface, the internal free surface within Cargo Hold 1 and the internal free surface of Cargo Hold 2, as defined in Figure 1.

Hence defining $F^{S_A S_B}_{kj}$ as the hydrodynamic radiation force or moment acting in the k^{th} direction on structure S_A, as a consequence of structure S_B moving in the j^{th} degree of freedom then Equations (1) may be generalised in the form:

$$F^{S_A S_B}_{kj}(\omega) = -A^{S_A S_B}_{kj}(\omega)\ddot{s}^{S_B}_j(\omega) - B^{S_A S_B}_{kj}(\omega)\dot{s}^{S_B}_j(\omega)$$
$$: \begin{cases} S_A, S_B \sim DS, FS_1 \text{ or } FS_2 \\ k, j = 1,2,\ldots,6 \end{cases} \quad (3a)$$

with

$$A^{S_A S_B}_{kj}(\omega) = \frac{\rho}{\omega s^{S_B}_{ja}}\iint_{S_A}\phi^j_{Im}\,n^{S_A}_k\,dS \text{ and}$$

$$B^{S_A S_B}_{kj}(\omega) = \frac{-\rho}{s^{S_B}_{ja}}\iint_{S_A}\phi^j_{Re}\,n^{S_A}_k\,dS. \quad (3b)$$

Hence $A^{S_A S_B}_{kj}(\omega)$ and $B^{S_A S_B}_{kj}(\omega)$ are the generalised added mass (inertia) and fluid damping coefficients. $n^{S_A}_k$ is the generalised k^{th} direction cosine associated with structure S_A. $\ddot{s}^{S_B}_j(\omega)$ & $\dot{s}^{S_B}_j(\omega)$ denote structural acceleration and velocity respectively on substructure S_B. The motion amplitude $s^{S_B}_{ja}$ can, without loss of generality, be assigned a value of unity when formulating the linearised fluid-structure interaction problem. That is, the values of $A^{S_A S_B}_{kj}(\omega)$ and $B^{S_A S_B}_{kj}(\omega)$, but not $F^{S_A S_B}_{kj}$, are independent of the values of $s^{S_B}_{ja}$.

Formulation of the radiation problems for the damaged ship is as for the intact ship, except the resulting velocity potential, and hence the associated radiation loadings, will reflect the presence of the stationary internal free surface(s). The radiation wave loadings due to the selected ship motion will invoke radiation forces and moments on the damaged ship and also the internal free surface(s). Similarly by invoking a required rigid body motion on a mass-less plate modelled free surface, assuming other free surface (if present) and damaged ship are assigned stationary boundary conditions, permits evaluation of the cross coupling on that free surface as well as the radiation loadings induced on the damaged ship and other free surface (if present). Whereas for a single intact ship 36 radiation loads per frequency must be calculated, a total of 216 different pairs of added mass and fluid damping coefficients must be determined for each wave frequency in the case of a hull with two internal free surfaces. Thus careful automated management of the data generated using Equations (3), a simple mathematical generalisation of Equation (1), is required.

It is only necessary in this paper to attribute heave, roll and pitch degrees of freedom to the horizontal flat plate modelled free surfaces, since only trivial normal velocity radiation boundary conditions exist for the surge, sway and yaw degrees of freedom. Consequently it follows that the selected motions to be invoked cannot induce non-zero fluid loadings on the internal free surfaces in the direction of the neglected motions.

The incident wave velocity potential is written as before. Since in the formulation of the diffraction problem all structures are treated as fixed it follows that the wave excitation forces and moments acting in the k^{th} direction on the structure S_A is readily determined from

$$F_k^{S_A} = -i\omega \iint_{S_A} \left[\Phi_I + \Phi_D\right] n_k^{S_A} \, dS$$
$$: k = 1, 2, \ldots, 6 \text{ and } S_A = DS, FS_1 \text{ or } FS_2 \qquad (4)$$

for each wave frequency ω and each wave heading β. The generation of wave loadings using Equations (3) & (4) to formulae the motion response equations will be designated 'simple' in Section 2.5.

The quality of the motion response analysis is both a function of the complexity of the equations formulated, and hence their ability to capture the true nature of the fluid structure interaction, and the quality of the velocity potentials used to determine the fluid loadings. The former aspect will be considered further in Section 3. The quality of the generated velocity potentials is to be addressed next.

2.4 QUALITY ASSESSMENT OF HYDRODYNAMIC MODELLING

As already indicated the effect of forward speed is not to be considered in the reported analysis. The principal goal of the reported research is to examine how the relative vertical motion at different locations on the first deck would be changed as a consequence of the introduced damage, given life boat deployment or boarding of specialists engineers from the sea might be the initial primary concern of the damage incurred. If forward speed were considered, in future extensions of the work, it would be more readily achieved implicitly in the processing of the hydrodynamic radiation and diffraction loads (see Tables 1 & 2 of Odabasi & Hearn (1977) for different alternative forward speed corrections for vertical and lateral motions using different theoretical models). If the forward speed were to be included in the 'kernel' of the linearised forward speed problem (whereby the interaction between the wave-making and radiation potentials is neglected) some analytical effort would be required to generalise the analysis to multi-body situations in which each substructure has its own degrees of freedom.

Here it is sufficient for the moment to recall the zero-speed Fredholm integral equation identity, namely

$$\alpha \phi_{P_i} = \iint_{S_W} \left[\phi \frac{\partial \psi}{\partial n} - \psi \frac{\partial \phi}{\partial n} \right] dS \quad : i = 1, 2, \ldots, N. \qquad (5a)$$

Equation (5a) can be used for the intact ship and the damage ship (with or without the inclusion of internal free surfaces) as outlined in Sections 2.2 and 2.3. The total number of boundary elements (N) indicated in Table 3 is simply the number of divisions the explicitly defined part of S_W is divided into. The integral equation 'kernel' ψ used in the MATTHEW software corresponds to alternative mathematically equivalent derived expressions of Hearn [1977] coupled with additional unpublished results for both infinite and finite water depth kernel. The general application of the integral equation identity (5a) is readily reduced to an equivalent algebraic system $A\phi = b$, where

$$\begin{bmatrix} A_{DS}^{DS} & A_{DS}^{FS_1} & A_{DS}^{FS_2} \\ A_{FS_1}^{DS} & A_{FS_1}^{FS_1} & A_{FS_1}^{FS_2} \\ A_{FS_2}^{DS} & A_{FS_2}^{FS_1} & A_{FS_2}^{FS_2} \end{bmatrix} \begin{bmatrix} \phi^{DS} \\ \phi^{FS_1} \\ \phi^{FS_2} \end{bmatrix} = \begin{bmatrix} b^{DS} \\ b^{FS_1} \\ b^{FS_2} \end{bmatrix}. \qquad (5b)$$

Here Equation (5b) is simultaneously addressing the coupled interaction between the distinct substructures of DS, FS_1 and FS_2. The removal of any internal free surface or the ultimate replacement of DS by IS in the case of an intact ship is readily achieved by removal of the zero submatrices and the unnecessary parts of the solution and boundary condition vectors ϕ and b of Equation (5b). Clearly, the influence matrix A exhibits all the required hydrodynamic cross coupling necessary.

The quality of the solution $\phi = \left[\phi^{DS} \quad \phi^{FS_1} \quad \phi^{FS_2}\right]^T$, or its obvious reductions, depends upon the numerical stability of the influence matrix A. Since geometric symmetry is not exploited for the intact ship, and doesn't exist for the other fluid structure interaction scenarios, a relevant measure of the quality of the solution ϕ is the relative error represented by the expression

$$\frac{\|\delta\phi\|}{\|\phi\|} \le \frac{\|A^{-1}\| \, \|A\|}{1 - \|A^{-1}\delta A\|} \left[\frac{\|\delta b\|}{\|b\|} + \frac{\|\delta A\|}{\|A\|} \right]. \qquad (6)$$

That is, the algebraic system $A\phi = b$ is assumed to take the form $(A + \delta A)(\phi + \delta\phi) = b + \delta b$ as a consequence of truncation and rounding errors in the numerical problem formulation. The usual matrix (vector) norm used with Equation (6) is the Euclidean norm. Defining the conditioning number of A as

$$K(A) = \frac{1}{N}\left\|A^{-1}\right\|\left\|A\right\| \qquad (7)$$

it follows that $K(I) = 1$ in the case of $A = I$, the unit matrix. Hence if $K(A)$ is large compared to unity the relative error in ϕ becomes less and less bounded according to Equation (6). The fluid structure interaction analysis MATTHEW, developed by the principal author, provides estimates of conditioning number for single and multi-bodied situations whether or not geometric symmetry is exploited. If the determined solution lacks mathematical integrity, concerning its numerical stability, as a consequence of formulating ill-conditioned equations, then the engineering analysis based on application of the determined solution will lack engineering analysis credibility too.

The production of ideal conditioning numbers corresponding to unity is a sought necessary condition, but it is not a sufficient condition to establish that the velocity potential solutions are acceptable for subsequent engineering analysis. It is possible to have idealistic conditioning numbers, but poor estimates of hydrodynamic cross coupling added mass (inertia) and fluid damping terms as a consequence of the number of boundary elements being too few and /or the distribution being inappropriate. In either case this means that the associated radiation and diffraction boundary conditions applied fail to capture the essential characteristics of the fluid structure interactions investigated.

To address this boundary element modelling aspect, the intact or damaged ship at zero forward speed must satisfy the readily established condition implied in Equation (1b), that is,

$$A_{kj}(\omega) = A_{jk}(\omega) \text{ and } B_{kj}(\omega) = B_{jk}(\omega) \text{ for all } j \text{ and } k \text{ for each frequency } \omega. \qquad (8)$$

Furthermore, the directly calculated wave excitation loads

$$F_k^{S_A\,\text{Direct}} = -i\omega\iint_{S_A}\left[\phi_I + \phi_D\right] n_k \, dS \, \exp(-i\omega t) \qquad (9a)$$

and the indirectly calculated Haskind [1954] wave excitation loads

$$F_k^{S_A\,\text{Haskind}} = \rho\iint_{S_A}\left[\phi_I \frac{\partial\phi^k}{\partial n} - \phi^k \frac{\partial\phi_I}{\partial n}\right] dS \exp(-i\omega t) \qquad (9b)$$

should yield the same answers, i.e. $F_k^{\text{Direct}} = F_k^{\text{Haskind}}$ for all directions k, all wave frequencies and wave headings. Other checks relating fluid damping and wave excitation are also available [Newman (1965)].

These cross checks have been applied to both the intact and damaged ship (without internal free surfaces) and only found to be lacking very marginally (less than 2%) in the sway-roll and roll-sway cross terms, see Appendix H of Saydan [2006] for plots of cross terms for intact and damaged ship. Increasing the number of facets was not considered worthwhile, as the predicted motions were insensitive to the sway-roll cross coupling term differences.

2.5 MOTION EQUATIONS FOR 'STRAIGHTFORWARD' AND 'SIMPLE' HYDRODYNAMIC MODELS

To compare the intact and damaged ship motions a sensible reference system *Oxyz* must be selected. Since a ship trims about the longitudinal centre of flotation then this point on the intact ship is selected as the global origin for all analyses. With the centre of gravity of the intact or damage ship designated as (X_{CG}, Y_{CG}, Z_{CG}), and the products of inertia being non-zero for the damaged ship, then the equations of motion based on the 'straightforward' fluid-structure interaction analysis, providing hydrodynamic loads using Equations (1b) & (2b), for surge, sway, heave, roll, pitch and yaw respectively are:

$$\frac{d}{dt}\left(M\dot{s}_1 - MY_{CG}\dot{s}_5 + MX_{CG}\dot{s}_6\right) = F_1 - \sum_{j=1}^{6}(A_{1j}\ddot{s}_j + B_{1j}\dot{s}_j)$$

$$\frac{d}{dt}\left(M\dot{s}_2 + MY_{CG}\dot{s}_4 - MZ_{CG}\dot{s}_6\right) = F_2 - \sum_{j=1}^{6}(A_{2j}\ddot{s}_j + B_{2j}\dot{s}_j)$$

$$\frac{d}{dt}\left(M\dot{s}_3 - MX_{CG}\dot{s}_4 + MZ_{CG}\dot{s}_5\right) = F_3 - \sum_{j=1}^{6}(A_{3j}\ddot{s}_j + B_{3j}\dot{s}_j) - \sum_{j=3,4,5} C_{3j}s_j$$

$$\frac{d}{dt}\left(I_{44}\dot{s}_4 + I_{45}\dot{s}_5 + I_{46}\dot{s}_6 - MY_{CG}\dot{s}_2 + MX_{CG}\dot{s}_3\right) = F_4 - \sum_{j=1}^{6}(A_{4j}\ddot{s}_j + B_{4j}\dot{s}_j) - \sum_{j=3,4,5} C_{4j}s_j$$

$$\frac{d}{dt}\left(I_{54}\dot{s}_4 + I_{55}\dot{s}_5 + I_{56}\dot{s}_6 + MY_{CG}\dot{s}_1 - MZ_{CG}\dot{s}_3\right) = F_5 - \sum_{j=1}^{6}(A_{5j}\ddot{s}_j + B_{5j}\dot{s}_j) - \sum_{j=3,4,5} C_{5j}s_j$$

$$\frac{d}{dt}\left(I_{64}\dot{s}_4 + I_{65}\dot{s}_5 + I_{66}\dot{s}_6 - MX_{CG}\dot{s}_1 + MZ_{CG}\dot{s}_2\right) = F_6 - \sum_{j=1}^{6}(A_{6j}\ddot{s}_j + B_{6j}\dot{s}_j). \qquad (10a)$$

The left hand side of Equations (10) represents the change in linear or angular momentum, for translations and rotational degrees of freedom respectively, and the right hand side provides the external forces and moments attributable to wave excitation, radiation loading and the Archimedean hydrostatic restoration influences (also determined by the MATTHEW software).

Recognising that for steady state harmonic solutions the velocity and accelerations are very simply related to the unknown motion displacements the coupled ordinary differential equations of Equations (10a) can be replaced by the equivalent algebraic system of simultaneous equations $As = F$. With $\left[M_{DS} + A_{DS}\right]$ and $\left[B_{DS}\right]$ denoting the sum of the usual mass-inertia and added mass matrices and the fluid damping matrix respectively, then

$$A = \begin{bmatrix} \left[C\right] - \omega^2\left[M_{DS} + A_{DS}\right] & \omega\left[B_{DS}\right] \\ -\omega\left[B_{DS}\right] & \left[C\right] - \omega^2\left[M_{DS} + A_{DS}\right] \end{bmatrix}. \quad \text{and}$$

$$\left[C\right] = \begin{bmatrix} 0 & 0 & 0 & 0 & 0 & 0 \\ 0 & 0 & 0 & 0 & 0 & 0 \\ 0 & 0 & C_{33} & C_{34} & C_{35} & 0 \\ 0 & 0 & C_{43} & C_{44} & C_{45} & 0 \\ 0 & 0 & C_{53} & C_{54} & C_{55} & 0 \\ 0 & 0 & 0 & 0 & 0 & 0 \end{bmatrix} \qquad (10b)$$

with s and F denoting column vectors of the unknown motion displacements and the corresponding wave excitation forces & moments respectively. Clearly each of the unknown displacements is complex and expressible as $s_j = s_{jRe} + i s_{jIm}$ with Re and Im denoting respectively the real and imaginary components. Thus the motion vector is defined as:

$$s = [s_{1Re}\ s_{1Im}\ s_{2Re}\ s_{2Im}\ s_{3Re}\ s_{3Im}\ s_{4Re}\ s_{4Im}\ s_{5Re}\ s_{5Im}\ s_{6Re}\ s_{6Im}]^T \qquad (10c)$$

with a similar expression for F. These motion equations may be directly solved analytically using Cramer's rule or solved numerically using a Gaussian elimination based process.

The motion responses generated from Equation (10b) are discussed in some detail in Saydan [2006], with Appendix J providing some 70 plots of the relative vertical motion of the ship at several distinct locations for different wave frequencies and wave headings, for both parent and optimised hull forms, for scenarios A to D defined in Table 1.

When modelling the internal free surfaces as 'mass-less' plates with heave, roll and pitch degrees of freedom the six equations of motion presented in Equation (10a), for the damaged ship, are readily generalised as follows:

$$\frac{d}{dt}\left(M\dot{s}_1^{DS} - MY_{CG}\dot{s}_5^{DS} + MX_{CG}\dot{s}_6^{DS}\right) = F_1^{DS} - \sum_{j=1}^{6}(A_{1j}^{DS\,DS}\ddot{s}_j^{DS} + B_{1j}^{DS\,DS}\dot{s}_j^{DS}) - \sum_{j=3,4,5}(A_{1j}^{DS\,FS_1}\ddot{s}_j^{FS_1} + B_{1j}^{DS\,FS_1}\dot{s}_j^{FS_1}) - \sum_{j=3,4,5}(A_{1j}^{DS\,FS_2}\ddot{s}_j^{FS_2} + B_{1j}^{DS\,FS_2}\dot{s}_j^{FS_2})$$

$$\frac{d}{dt}\left(M\dot{s}_2^{DS} + MY_{CG}\dot{s}_4^{DS} - MZ_{CG}\dot{s}_6^{DS}\right) = F_2^{DS} - \sum_{j=1}^{6}(A_{2j}^{DS\,DS}\ddot{s}_j^{DS} + B_{2j}^{DS\,DS}\dot{s}_j^{DS}) - \sum_{j=3,4,5}(A_{2j}^{DS\,FS_1}\ddot{s}_j^{FS_1} + B_{2j}^{DS\,FS_1}\dot{s}_j^{FS_1}) - \sum_{j=3,4,5}(A_{2j}^{DS\,FS_2}\ddot{s}_j^{FS_2} + B_{2j}^{DS\,FS_2}\dot{s}_j^{FS_2})$$

$$\frac{d}{dt}\left(M\dot{s}_3^{DS} - MX_{CG}\dot{s}_4^{DS} + MZ_{CG}\dot{s}_5^{DS}\right) = F_3^{DS} - \sum_{j=1}^{6}(A_{3j}^{DS\,DS}\ddot{s}_j^{DS} + B_{3j}^{DS\,DS}\dot{s}_j^{DS}) - \sum_{j=3,4,5}C_{3j}^{DS\,DS}s_j^{DS} - \sum_{j=3,4,5}(A_{3j}^{DS\,FS_1}\ddot{s}_j^{FS_1} + B_{3j}^{DS\,FS_1}\dot{s}_j^{FS_1}) - \sum_{j=3,4,5}(A_{3j}^{DS\,FS_2}\ddot{s}_j^{FS_2} + B_{3j}^{DS\,FS_2}\dot{s}_j^{FS_2})$$

$$\frac{d}{dt}\left(I_{44}\dot{s}_4^{DS} + I_{45}\dot{s}_5^{DS} + I_{46}\dot{s}_6^{DS} - MY_{CG}\dot{s}_2^{DS} + MX_{CG}\dot{s}_3^{DS}\right) = F_4^{DS} - \sum_{j=1}^{6}(A_{4j}^{DS\,DS}\ddot{s}_j^{DS} + B_{4j}^{DS\,DS}\dot{s}_j^{DS}) - \sum_{j=3,4,5}C_{4j}^{DS\,DS}s_j^{DS} - \sum_{j=3,4,5}(A_{4j}^{DS\,FS_1}\ddot{s}_j^{FS_1} + B_{4j}^{DS\,FS_1}\dot{s}_j^{FS_1}) - \sum_{j=3,4,5}(A_{4j}^{DS\,FS_2}\ddot{s}_j^{FS_2} + B_{4j}^{DS\,FS_2}\dot{s}_j^{FS_2})$$

$$\frac{d}{dt}\left(I_{54}\dot{s}_4^{DS} + I_{55}\dot{s}_5^{DS} + I_{56}\dot{s}_6^{DS} + MY_{CG}\dot{s}_1^{DS} - MZ_{CG}\dot{s}_3^{DS}\right) = F_5^{DS} - \sum_{j=1}^{6}(A_{5j}^{DS\,DS}\ddot{s}_j^{DS} + B_{5j}^{DS\,DS}\dot{s}_j^{DS}) - \sum_{j=3,4,5}C_{5j}^{DS\,DS}s_j^{DS} - \sum_{j=3,4,5}(A_{5j}^{DS\,FS_1}\ddot{s}_j^{FS_1} + B_{5j}^{DS\,FS_1}\dot{s}_j^{FS_1}) - \sum_{j=3,4,5}(A_{5j}^{DS\,FS_2}\ddot{s}_j^{FS_2} + B_{5j}^{DS\,FS_2}\dot{s}_j^{FS_2})$$

$$\frac{d}{dt}\left(I_{64}\dot{s}_4^{DS} + I_{65}\dot{s}_5^{DS} + I_{66}\dot{s}_6^{DS} - MX_{CG}\dot{s}_1^{DS} + MZ_{CG}\dot{s}_2^{DS}\right) = F_6^{DS} - \sum_{j=1}^{6}(A_{6j}^{DS\,DS}\ddot{s}_j^{DS} + B_{6j}^{DS\,DS}\dot{s}_j^{DS}) - \sum_{j=3,4,5}(A_{6j}^{DS\,FS_1}\ddot{s}_j^{FS_1} + B_{6j}^{DS\,FS_1}\dot{s}_j^{FS_1}) - \sum_{j=3,4,5}(A_{6j}^{DS\,FS_2}\ddot{s}_j^{FS_2} + B_{6j}^{DS\,FS_2}\dot{s}_j^{FS_2}).$$

(11a)

The additional motion equations for the mass-less plate modelled free surface(s) for their associated heave, roll and pitch degrees of freedom for damaged ship scenario A (generated in a manner exactly analogous to the ship motion equations) yield the following relationships:

$$
\begin{aligned}
0 = F_3^{FS_2} &- \sum_{j=3,4,5} (A_{3j}^{FS_2\,FS_2}\ddot{s}_j^{FS_2} + B_{3j}^{FS_2\,FS_2}\dot{s}_j^{FS_2}) \\
&- \sum_{j=3,4,5} C_{3j}^{FS_2\,FS_2} s_j^{FS_2} \\
&- \sum_{j=3,4,5} (A_{3j}^{FS_2\,FS_1}\ddot{s}_j^{FS_1} + B_{3j}^{FS_2\,FS_1}\dot{s}_j^{FS_1}) \\
&- \sum_{j=1}^{6} (A_{3j}^{FS_2\,DS}\ddot{s}_j^{DS} + B_{3j}^{FS_2\,DS}\dot{s}_j^{DS}) \\
0 = F_4^{FS_2} &- \sum_{j=1}^{6} (A_{4j}^{FS_2\,FS_2}\ddot{s}_j^{FS_2} + B_{4j}^{FS_2\,FS_2}\dot{s}_j^{FS_2}) \\
&- \sum_{j=3,4,5} C_{4j}^{FS_2\,FS_2} s_j^{FS_2} \\
&- \sum_{j=3,4,5} (A_{4j}^{FS_2\,FS_1}\ddot{s}_j^{FS_1} + B_{4j}^{FS_2\,FS_1}\dot{s}_j^{FS_1}) \\
&- \sum_{j=1}^{6} (A_{4j}^{FS_2\,DS}\ddot{s}_j^{DS} + B_{4j}^{FS_2\,DS}\dot{s}_j^{DS}) \\
0 = F_5^{FS_2} &- \sum_{j=1}^{6} (A_{5j}^{FS_2\,FS_2}\ddot{s}_j^{FS_2} + B_{5j}^{FS_2\,FS_2}\dot{s}_j^{FS_2}) - \sum_{j=3,4,5} C_{5j}^{FS_2\,FS_2} s_j^{FS_2} \\
&- \sum_{j=3,4,5} (A_{4j}^{FS_2\,FS_2}\ddot{s}_j^{FS_1} + B_{4j}^{FS_2\,FS_1}\dot{s}_j^{FS_1}) \\
&- \sum_{j=1}^{6} (A_{5j}^{FS_2\,DS}\ddot{s}_j^{DS} + B_{5j}^{FS_2\,DS}\dot{s}_j^{DS})
\end{aligned}
\qquad (11b)
$$

Clearly in Equations (11b) there is no linear or angular momentum for the mass-less internal free-surface model for hold 2. When scenario C is considered there are 3 more similar equations of the same form, namely:

$$
\begin{aligned}
0 = F_3^{FS_1} &- \sum_{j=3,4,5} (A_{3j}^{FS_1\,FS_1}\ddot{s}_j^{FS_1} + B_{3j}^{FS_1\,FS_1}\dot{s}_j^{FS_1}) - \sum_{j=3,4,5} C_{3j}^{FS_1\,FS_1} s_j^{FS_1} \\
&- \sum_{j=3,4,5} (A_{3j}^{FS_1\,FS_2}\ddot{s}_j^{FS_2} + B_{3j}^{FS_1\,FS_2}\dot{s}_j^{FS_2}) \\
&- \sum_{j=1}^{6} (A_{3j}^{FS_1\,DS}\ddot{s}_j^{DS} + B_{3j}^{FS_1\,DS}\dot{s}_j^{DS}) \\
0 = F_4^{FS_1} &- \sum_{j=1}^{6} (A_{4j}^{FS_1\,FS_1}\ddot{s}_j^{FS_1} + B_{4j}^{FS_1\,FS_1}\dot{s}_j^{FS_1}) - \sum_{j=3,4,5} C_{4j}^{FS_1\,FS_1} s_j^{FS_1} \\
&- \sum_{j=3,4,5} (A_{4j}^{FS_1\,FS_2}\ddot{s}_j^{FS_2} + B_{4j}^{FS_1\,FS_2}\dot{s}_j^{FS_2}) \\
&- \sum_{j=1}^{6} (A_{4j}^{FS_1\,DS}\ddot{s}_j^{DS} + B_{4j}^{FS_1\,DS}\dot{s}_j^{DS}) \\
0 = F_5^{FS_1} &- \sum_{j=1}^{6} (A_{5j}^{FS_1\,FS_1}\ddot{s}_j^{FS_1} + B_{5j}^{FS_1\,FS_1}\dot{s}_j^{FS_1}) - \sum_{j=3,4,5} C_{5j}^{FS_1\,FS_1} s_j^{FS_1} \\
&- \sum_{j=3,4,5} (A_{4j}^{FS_1\,FS_2}\ddot{s}_j^{FS_2} + B_{4j}^{FS_1\,FS_2}\dot{s}_j^{FS_2}) \\
&- \sum_{j=1}^{6} (A_{5j}^{FS_1\,DS}\ddot{s}_j^{DS} + B_{5j}^{FS_1\,DS}\dot{s}_j^{DS})
\end{aligned}
\qquad (11c)
$$

Equations (11a) to (11c) are again merged into an equivalent set of simultaneous algebraic equations of the form $As = F$, subject to mathematical mode defined in Equation (11d).

The size of the submatrices in Equation (11d) is not uniform and hence the size for each is provided in the general form $n \times m$ under each contributing term.

The hydrostatic influence matrix $[C]$ and related hydrostatic stiffness sub-matrices having the general form of Equation (11e) with the subscripts and superscripts designated *' Blank '* to indicate that just one of the possible substructure designations DS, FS_1 or FS_2 must be considered, since there is no hydrostatic coupling between the substructures.

At this stage one may therefore address the intact and damaged ship using the formulation of Equations (10) or extend the damaged ship model to that of Equations (11). Both sets of equations are readily solved using Gaussian elimination. Furthermore just as the hydrodynamic formulations are checked for conditioning numbers so was Equation (11d). They were found to be extremely stable.

$$
A = \begin{bmatrix}
[C] - \omega^2 \begin{bmatrix} [M_{DS} + A_{DS1}]_{6x6} & [A_{FS11}]_{6x3} & [A_{FS21}]_{6x3} \\ [A_{DS2}]_{3x6} & [A_{FS12}]_{3x3} & [A_{FS22}]_{3x3} \\ [A_{DS3}]_{3x6} & [A_{FS13}]_{3x3} & [A_{FS23}]_{3x3} \end{bmatrix} & \omega. \begin{bmatrix} [B_{DS1}]_{6x6} & [B_{FS11}]_{6x3} & [B_{FS21}]_{6x3} \\ [B_{DS2}]_{3x6} & [B_{FS12}]_{3x3} & [B_{FS22}]_{3x3} \\ [B_{DS3}]_{3x6} & [B_{FS13}]_{3x3} & [B_{FS23}]_{3x3} \end{bmatrix} \\
-\omega. \begin{bmatrix} [B_{DS1}]_{6x6} & [B_{FS11}]_{6x3} & [B_{FS21}]_{6x3} \\ [B_{DS2}]_{3x6} & [B_{FS12}]_{3x3} & [B_{FS22}]_{3x3} \\ [B_{DS3}]_{3x6} & [B_{FS13}]_{3x3} & [B_{FS23}]_{3x3} \end{bmatrix} & [C] - \omega^2 \begin{bmatrix} [M_{DS} + A_{DS1}]_{6x6} & [A_{FS11}]_{6x3} & [A_{FS21}]_{6x3} \\ [A_{DS2}]_{3x6} & [A_{FS12}]_{3x3} & [A_{FS22}]_{3x3} \\ [A_{DS3}]_{3x6} & [A_{FS13}]_{3x3} & [A_{FS23}]_{3x3} \end{bmatrix}
\end{bmatrix}
\qquad (11d)
$$

$$[C] = \begin{bmatrix} 0 & 0 & 0 & 0 & 0 & 0 & 0 & 0 & 0 & 0 & 0 & 0 \\ 0 & 0 & 0 & 0 & 0 & 0 & 0 & 0 & 0 & 0 & 0 & 0 \\ 0 & 0 & & & & 0 & 0 & 0 & 0 & 0 & 0 & 0 \\ 0 & 0 & & \left[C_{DS}\right]_{3x3} & & 0 & 0 & 0 & 0 & 0 & 0 & 0 \\ 0 & 0 & & & & 0 & 0 & 0 & 0 & 0 & 0 & 0 \\ 0 & 0 & 0 & 0 & 0 & 0 & 0 & 0 & 0 & 0 & 0 & 0 \\ 0 & 0 & 0 & 0 & 0 & 0 & & & & 0 & 0 & 0 \\ 0 & 0 & 0 & 0 & 0 & 0 & \left[C_{FS1}\right]_{3x3} & & & 0 & 0 & 0 \\ 0 & 0 & 0 & 0 & 0 & 0 & & & & 0 & 0 & 0 \\ 0 & 0 & 0 & 0 & 0 & 0 & 0 & 0 & 0 & & & \\ 0 & 0 & 0 & 0 & 0 & 0 & 0 & 0 & 0 & \left[C_{FS2}\right]_{3x3} & & \\ 0 & 0 & 0 & 0 & 0 & 0 & 0 & 0 & 0 & & & \end{bmatrix}$$

$$\left[C_{Blank}\right]_{3\times3} = \begin{bmatrix} C_{33}^{Blank\ Blank} & C_{34}^{Blank\ Blank} & C_{35}^{Blank\ Blank} \\ C_{43}^{Blank\ Blank} & C_{44}^{Blank\ Blank} & C_{45}^{Blank\ Blank} \\ C_{53}^{Blank\ Blank} & C_{54}^{Blank\ Blank} & C_{55}^{Blank\ Blank} \end{bmatrix} \quad (11e)$$

Some readers might consider Equations (11) are unnecessarily complex. However, analyses completed indicate that attributing three degrees of motion to the free surfaces is necessary because if one simply assumes that heave is the only degree of freedom of any importance then the predicted relative vertical motions of the internal free surfaces were found to be excessive, being far greater than the clearance between the undisturbed free surface and the deck above the internal free surface! Attributing heave, roll and pitch degrees of freedom to the internal free surface and assuming only hydrostatic restoration terms are important also provides larger motions of the internal free surfaces than expected, but they are not as excessive as the relative motions of a single degree of freedom attributed internal free surface. Therefore simply extending the degrees of freedom in the motion equations of Equation (11) is insufficient.

Since Equations (11) do not recognise the air within the hold above the free surface(s), modelled as a mass-less 'plate', the next level of generalisation needs to include the internal free surface related air springs of Figure 3.

The next section looks at different methods of determining the stiffness of the air springs prior to presenting further generalisations of Equations (11) to improve the modelling of the damaged ship motions.

3. ESTIMATING THE STIFFNESS PROPERTY OF THE IN-HOLD AIR

The stiffness of the air is now estimated using a number of different methods of varying complexity. For total generality the air above the internal free surface, within a damaged hold, is assumed to be adiabatic reversible (isentropic). Hence the governing pressure - volume relationship is $PV^{\gamma} = P_o V_o^{\gamma}$. Furthermore, assuming that for any particular selected cargo hold the still water plane cross sectional area is A_o, the wall-sided nature of the holds implies the cross sectional area is approximately constant throughout and thus $V_0 = y_0 A_0$, where y_o is average height of air gap between undisturbed internal free surface and deck. With these simple assumptions alternative derivations of the air stiffness are now presented.

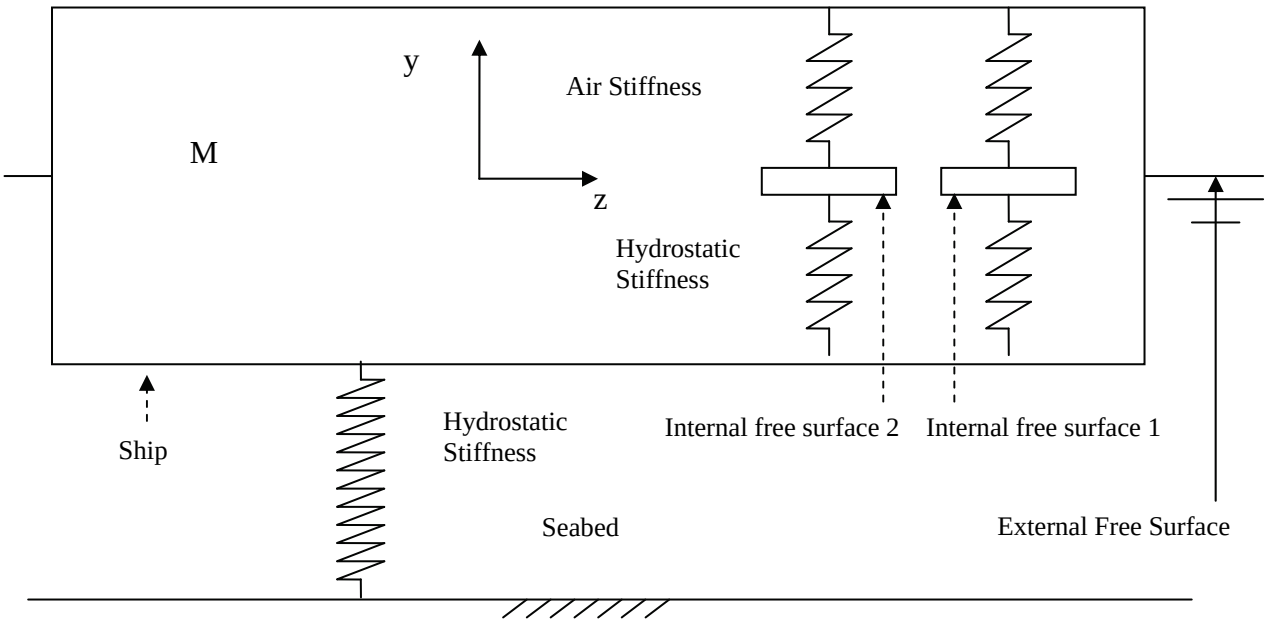

Figure 3 - Schematic Presentation of Damaged Ship and Internal Free Surfaces

3.1 A SIMPLE LINEAR DISPLACEMENT MODEL

For an upward uniform movement of the internal free surface y it follows that $V=(y_0-y)A_0$. The free surface as a result of its change in position will experience both a hydrostatic force (already dealt with) and an as yet undetermined 'aerostatic' force. Let the latter force be denoted by $F=PA_o$, or writing $P=F/A_o$ it follows that:

$$PV^\gamma=\frac{F}{A_o}(y_o-y)^\gamma A_o^\gamma=P_oA_o^\gamma y_o^\gamma.$$

This implies that $F=P_oA_o\dfrac{y_o^\gamma}{(y_o-y)^\gamma}$ and hence $F_o=P_oA_o\dfrac{y_o^\gamma}{y_o^\gamma}$ by definition. Thus the change in 'aerostatic' force due to the vertical movement y is:

$$\Delta F_{air}=F-F_o=P_oA_oy_o^\gamma\left\{\frac{1}{(y_o-y)^\gamma}-\frac{1}{y_o^\gamma}\right\}=K_{air}\,y\text{, say.} \tag{12}$$

Thus the air-stiffness equates to:

$$\begin{aligned}K_{air}(y)&=\frac{P_0A_0y_0^\gamma}{y}\left\{\frac{1}{(y_0-y)^\gamma}-\frac{1}{y_0^\gamma}\right\}\\&=\frac{P_0A_0\left(y_0^\gamma-(y_0-y)^\gamma\right)}{y(y_0-y)^\gamma}.\end{aligned} \tag{13a}$$

Assuming the peak vertical amplitude of the free surface is y_{peak}, the average air-stiffness corresponds to:

$$K_{air}=\overline{K_{air}(y)}=\frac{1}{2y_{peak}}\int_{-y_{peak}}^{y_{peak}}\frac{P_oA_o\left(y_o^\gamma-(y_o-y)^\gamma\right)}{y(y_o-y)^\gamma}\,dy. \tag{13b}$$

Consultation of Gradshteyn and Ryzhik (1965) did not yield a closed form analytic integration for general γ, although closed form integration is straightforward for $\gamma=1$. Otherwise knowing that $|y|\le y_{peak}<y_o$ Equation (13b) is written as:

$$K_{air}=\overline{K_{air}(y)}=\frac{P_oA_o}{2y_{peak}}\int_{-y_{peak}}^{y_{peak}}\frac{1}{y}\left[\left(1-\frac{y}{y_o}\right)^{-\gamma}-1\right]dy. \tag{13c}$$

Applying the Binomial Theorem yields the general expression:

$$K_{air}=\frac{P_oV_o}{2y_o^2y_{peak}}\int_{-y_{peak}}^{y_{peak}}\left[\begin{array}{l}\gamma+\dfrac{\gamma(\gamma+1)}{2!}\left(\dfrac{y}{y_o}\right)+\ldots\\+\dfrac{\gamma(\gamma+1)\ldots(\gamma+n-1)}{n!}\left(\dfrac{y}{y_o}\right)^{n-1}\ldots\end{array}\right]dy$$

and undertaking implied integration leads to

$$\begin{aligned}K_{air}=\frac{P_oV_0}{y_o^2}\Bigg[&\gamma+\frac{\gamma(\gamma+1)(\gamma+2)}{3\,3!}\left(\frac{y}{y_o}\right)^2\\&+\frac{\gamma(\gamma+1)(\gamma+2)(\gamma+3)(\gamma+4)}{5\,5!}\left(\frac{y}{y_o}\right)^4+\ldots\\&+\frac{\gamma(\gamma+1)(\gamma+2)\ldots(\gamma+2n-1)(\gamma+2n+2)}{(2n+1)\,(2n+1)!}\left(\frac{y}{y_o}\right)^{2n}+\ldots\Bigg].\end{aligned} \tag{13d}$$

Application of the ratio test for a series of positive terms (T_n), see Gow [1964], establishes that the series presented is convergent since $p=(y/y_o)^2<1$ and

$$\lim_{n\to\infty}\frac{T_{n+1}}{T_n}=\frac{\left(1+\dfrac{\gamma+1}{2n}\right)\left(1+\dfrac{\gamma+1}{2n+1}\right)}{\left(1+\dfrac{2}{2n-1}\right)}\left(\frac{y}{y_o}\right)^2\to p<1.$$

Since y_{peak} is not known a' priori then the air stiffness of Equation (13d) will have to be determined iteratively. Ideally the series ought to be truncated only when the relative error of the neglected terms is sufficiently small.

Neglecting terms above second order in Equation (13d) yields the simplest possible isothermal air stiffness estimate, namely that $K_{air}=\gamma\dfrac{P_0V_0}{y_0^2}=\gamma K_{air}^T$, where $K_{air}^T=\left.\dfrac{dF}{dy}\right|_{\substack{\gamma=1\\y=0}}=\dfrac{P_oV_o}{y_o^2}$ is determined from Equation (12). That is, assuming the free surface motion is not significant K_{air}^T is readily equated to the slope of the force curve at the origin.

Rather than commit to a second iterative process within the motion equation iteration process, if the stiffness estimation of Equation (13d) is used, an alternative procedure based on energy argument is presented next.

3.2 A SIMPLE ENERGY STORAGE DISPLACEMENT MODEL

Essentially the energy needed to displace the internal free surface from $-y_{peak}$ to y_{peak} is the same as the energy stored in a spring for the same displacement. For the

positive displacement, upon appealing to Equation (12), it follows that:

$$\int_0^{y_{peak}} K_{air}^{+} y\,dy = \int_0^{y_{peak}} \Delta F_{air}\,dy \text{ or } \frac{1}{2}K_{air}^{+} y_{peak}^2 = \int_0^{y_{peak}} P_o A_o y_o^{\gamma}\left(\frac{1}{(y_o - y)^{\gamma}} - \frac{1}{y_o^{\gamma}}\right)dy.$$

This integrand is more readily processed than that of Equation (13b) and consequently

$$K_{air}^{+} = \frac{2P_o A_o y_o^{\gamma}}{y_{peak}^2}\int_0^{y_{peak}}\left(\frac{1}{(y_0 - y)^{\gamma}} - \frac{1}{y_0^{\gamma}}\right)dy$$

$$= \frac{2P_0 A_0 y_0^{\gamma}}{y_{peak}^2}\left(\frac{(y_0 - y_{peak})y_0^{\gamma} - y_0(y_0 - y_{peak})^{\gamma}}{(\gamma - 1)y_0^{\gamma}(y_0 - y_{peak})^{\gamma}} - \frac{y_{peak}}{y_0^{\gamma}}\right). \quad (14a)$$

The corresponding result for the negative part of the free surface displacement is:

$$\int_{-y_{peak}}^{0} K_{air}^{-} y\,dy = \int_{-y_{peak}}^{0} \Delta F_{air}\,dy \quad \text{or}$$

$$\frac{1}{2}K_{air}^{-} y_{peak}^2 = \int_0^{-y_{peak}} P_o A_o y_o^{\gamma}\left(\frac{1}{(y_o - y)^{\gamma}} - \frac{1}{y_o^{\gamma}}\right)dy$$

and rearranging leads to

$$K_{air}^{-} = \frac{2P_o A_o y_o^{\gamma}}{y_{peak}^2}\left(\frac{(y_o + y_{peak})y_o^{\gamma} - y_o(y_o + y_{peak})^{\gamma}}{(\gamma - 1)y_o^{\gamma}(yo + y_{peak})^{\gamma}} + \frac{y_{peak}}{y_0^{\gamma}}\right), \quad (14b)$$

and upon averaging Equations (14a) & (14b) it follows that

$$K_{air} = \frac{K_{air}^{+} + K_{air}^{-}}{2} = \frac{P_o A_o y_o^{\gamma}}{y_{peak}^2(\gamma - 1)}\left(\frac{1}{(y_0 - y_{peak})^{\gamma - 1}} + \frac{1}{(y_0 + y_{peak})^{\gamma - 1}} - \frac{2}{y_0^{\gamma - 1}}\right). \quad (14c)$$

The expressions for K_{air} provided by Equations (13a), (13d) & (14c) may be applied for any selected value of γ.

In all cases evaluation of the stiffness is dependent upon the equilibrium pressure P_o and the air gap y_o between internal free surface and deck.

In this section and the previous section the air stiffness was determined assuming an equilibrium pressure P_0 and a maximum gap between the internal free surface and the deck of y_0. The ship was essentially assumed (albeit implicitly) to be in its static equilibrium position. The next step is to consider the influence of the ship motion upon the air stiffness. This will permit appropriate generalisation of the motion response equations presented in Section 3.6.

3.3 GENERALISATION OF AIR STIFFNESS COEFFICIENT TO REFLECT SHIP MOTION

The hole in the hull is assumed to remain below the external free surface, as indicated by the ship damage statistics considered and applied, and as illustrated in Figure 4.

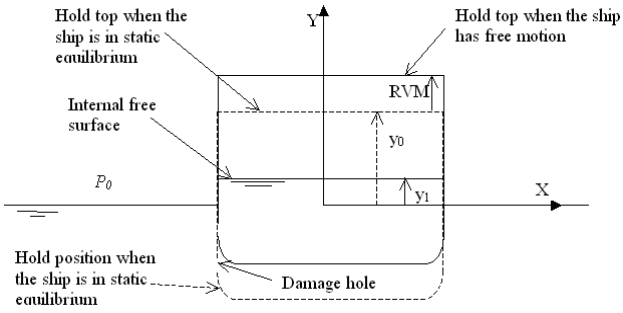

Figure 4 – Scheme to generalise hold stiffness due to ship relative vertical motion

The existence of the hole and the motion of the ship suggest that the mean position of the internal free surface is unlikely to remain at its static equilibrium position of $y = Y = 0$, but may assume a new mean position $Y = y_1$ as a consequence of the phasing of the motion of the internal free surface and the ship. The consequence of this change in mean internal free surface position leads to the following arguments regarding air stiffness.

Equilibrium pressure P_{eq} in the hold for an isentropic transformation of an ideal gas satisfies $P_o V_o^{\gamma} = P_{eq} V_{eq}^{\gamma}$. Assuming, as before, that $V_o = A_o y_o$ then

$$P_o y_o^{\gamma} = P_{eq} y_{eq}^{\gamma} \quad (15a)$$

and it follows from Figure 4 that

$$y_{eq} = y_0 + RVM - y_1 \text{ and}$$

$$\text{hence } P_{eq} = P_0\left(\frac{y_0}{y_0 + RVM - y_1}\right)^{\gamma}. \quad (15b, c)$$

The internal pressure at Y=0 is the same as the external atmospheric pressure P_0. When the internal free surface is at Y= y_1 then the pressure of the air in the hold is given by P_{eq} defined by Equation (15c). On the other hand the pressure due to the column of water of height y_1

is $\rho.g.y_1$. Hence equilibrium of pressure in the hold at Y=0, equal to the pressure outside the hold, because the damage hole in the hold maintains pressure equilibrium, requires that $P_0 = P_{eq} + \rho g y_1$, or, equivalently

$$P_o = P_o\left(\frac{y_o}{y_o + RVM - y_1}\right)^{\gamma} + \rho\, g\, y_1. \qquad (16)$$

Equation (16), a transcendental equation, is necessary. It must be solved for y_1, for a given air gap y_o and an estimated magnitude of the resultant vertical motion of ship, RVM. This last quantity is to be determined at the selected representative point for the internal free surface, the centroid of the internal free surface, say.

3.3(a) Solutions of internal free surface location y_1

Initially consider the simpler isothermal case of $\gamma = 1$, for which y_1 is denoted by y_1^T. In this case Equation (16) leads to the quadratic equation

$$y_1^{T2}\,\rho g - y_1^T\left(P_0 + \rho g\left(y_0 + RVM\right)\right) + P_0 RVM = 0 \qquad (17)$$

and the required meaningful solution is

$$y_1^T = \frac{P_0 + \rho g\left(y_0 + RVM\right) - \sqrt{\left(P_0 + \rho g\left(y_0 + RVM\right)\right)^2 - 4\rho g P_0 RVM}}{2\rho g} \qquad (18)$$

since, for no relative vertical motion (RVM=0), the only physically acceptable solution is $y_1^T = 0$.

In general, for $\gamma \neq 1$, Equation (16) must be solved for y_1. The variation of y_1 as a function of RVM is illustrated in Figure 5. The influence of γ is not particularly significant.

Calculation of y_1 for isentropic and isothermal conditions

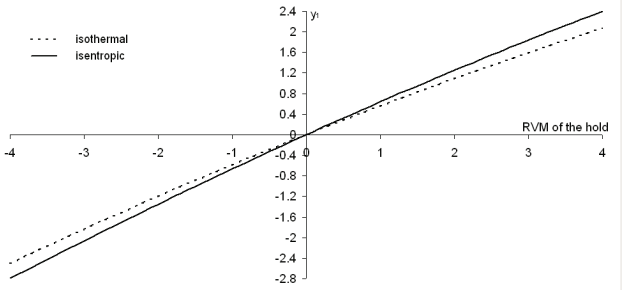

Figure 5 - Variation of mean position of internal free surface with ship relative vertical motion (RVM)

3.3(b) Final Specification of Air Stiffness Coefficients

The next step is to extend the motion response equations provided initially as Equations (11) of Section 2.5, assuming the generalised fluid-structure interaction analysis of Section 2.3, so that the influences of the internal free surface air stiffness is included in a sensible manner. By sensible one means that the expressions explicitly used should be consistent with the modelling of the hydrodynamic cross coupling between ship & free surface and free surface & ship.

When considering the hydrodynamic loads on an internal free surface the ship is considered stationary, therefore when considering the air stiffness on the internal free surface it is suggested that the notation of the air stiffness expression of Equation (14c), the physically most representative model, is now written as:

$$K_{air}^{FS_i} = \frac{P_0 A_o^{FS_i}\, y_o^{FS_i\,\gamma}}{y_{peak}^{FS_i\,2}\left(\gamma - 1\right)}\left(\begin{array}{l}\dfrac{1}{\left(y_o^{FS_i} - y_{peak}^{FS_i}\right)^{\gamma-1}} + \\ + \dfrac{1}{\left(y_o^{FS_i} + y_{peak}^{FS_i}\right)^{\gamma-1}} - \dfrac{2}{y_o^{FS_i\,\gamma-1}}\end{array}\right) \text{:i=1\&2} \qquad (19a)$$

When considering the influence of the internal free surface on the moving ship it is then suggested that Equation (19a) is further generalised to take on the form:

$$K_{air}^{DS\,FS_i} = \frac{P_{eq}^{FS_i} A_o^{FS_i}\, y_{eq}^{FS_i\,\gamma}}{y_{peak}^{FS_i\,2}\left(\gamma - 1\right)}\left(\begin{array}{l}\dfrac{1}{\left(y_{eq}^{FS_i} - y_{peak}^{FS_i}\right)^{\gamma-1}} + \\ + \dfrac{1}{\left(y_{eq}^{FS_i} + y_{peak}^{FS_i}\right)^{\gamma-1}} - \dfrac{2}{y_{eq}^{FS_i\,\gamma-1}}\end{array}\right)$$

i=1 & 2, (19b)

subject to $P_{eq}^{FS_i} = P_0\left(\dfrac{y_o^{FS_i}}{y_o^{FS_i} + RVM_{FS_i}^{DS} - y_1^{FS_i}}\right)^{\gamma}$ and

$$y_{eq}^{FS_i} = y_o^{FS_i} + RVM_{FS_i}^{DS} - y_1^{FS_i}. \qquad (19c)$$

That is, the left-hand side superscripts $DS\ FS_i$ indicate that the damaged ship is being influenced by the i[th] free surface. As already noted the internal free surface is FS_2 in scenario A and free surfaces FS_2 & FS_1 in scenario C.

Equations (19) are thus appropriate applications of the air stiffness based upon the ideas of Section 3.2, rather than the simpler linear displacement model of Section 3.1 However, when applying Equation (19b) it is necessary to be able to cope with the dependence of the air stiffness upon the unknown internal free surface offset y_1 and the vertical relative motion (RVM) of the ship. The y_{peak}

value comes from the modulus of the heave amplitude for the wave frequency being considered. Clearly the motion response equations must be solved by iteration.

However, there are at most 4 distinct air stiffness terms to be appropriately included in the extended governing equations of motion considered next.

4 MODELLING MOTION RESPONSES OF DAMAGED SHIP AND INTERNAL FREE SURFACES

The total number of equations of motion will vary from six for the damage ship in isolation to nine or twelve according as the influence of one (Scenario A) and then two (Scenario C) internal free surfaces are included in the hydrodynamic analysis and dynamic motion analysis. To appreciate how the different air stiffness terms of the previous section are included consider the schematic interactions illustrated in Figure 2 together with the levers l_i between the ith free surface and the system origin (located at the 'intact' centre of flotation). The levers l_i are superimposed on the discretised damaged-ship of Figure 6.

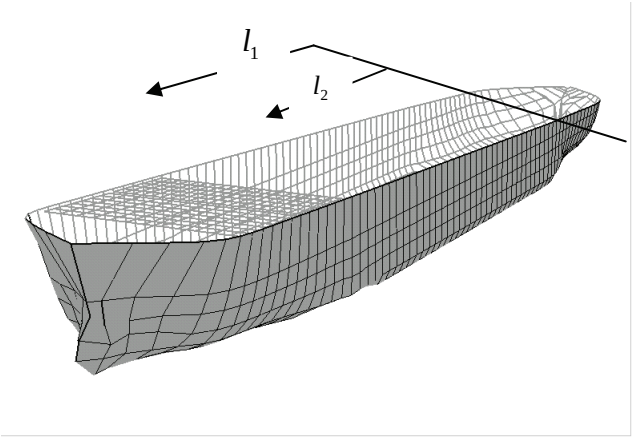

Figure 6 - Damaged Derbyshire model and definitions of levers from LCF to different free surfaces

It follows that just the six heave and pitch motion equations of Equations (11a, 11b & 11c) need to be generalised to include the internal hydrostatic and air stiffness terms. Only these six modified equations are presented in Equations (20), the other six equations remain unchanged.

The modified heave and pitch equations for scenario C now assume the form:

$$\frac{d}{dt}\left(M\dot{s}_3^{DS} - MX_{CG}\dot{s}_4^{DS} + MZ_{CG}\dot{s}_5^{DS}\right) = F_3^{DS}$$
$$-\sum_{j=1}^{6}(A_{3j}^{DS\,DS}\ddot{s}_j^{DS} + B_{3j}^{DS\,DS}\dot{s}_j^{DS}) - \sum_{j=3,4,5} C_{3j}^{DS\,DS}s_j^{DS}$$
$$-\sum_{j=3,4,5}(A_{3j}^{DS\,FS_1}\ddot{s}_j^{FS_1} + B_{3j}^{DS\,FS_1}\dot{s}_j^{FS_1})$$
$$-\sum_{j=3,4,5}(A_{3j}^{DS\,FS_2}\ddot{s}_j^{FS_2} + B_{3j}^{DS\,FS_2}\dot{s}_j^{FS_2})$$
$$-K_{air}^{DS\,FS_1}\left[s_3^{DS} - l_1 s_5^{DS} - s_3^{FS_1} + l_1 s_5^{FS_1}\right]$$
$$-K_{air}^{DS\,FS_2}\left[s_3^{DS} - l_2 s_5^{DS} - s_3^{FS_2} + l_2 s_5^{FS_2}\right],$$

$$\frac{d}{dt}\left(I_{54}\dot{s}_4^{DS} + I_{55}\dot{s}_5^{DS} + I_{56}\dot{s}_6^{DS} + MY_{CG}\dot{s}_1^{DS} - MZ_{CG}\dot{s}_3^{DS}\right)$$
$$= F_5^{DS} - \sum_{j=1}^{6}(A_{5j}^{DS\,DS}\ddot{s}_j^{DS} + B_{5j}^{DS\,DS}\dot{s}_j^{DS}) - \sum_{j=3,4,5} C_{5j}^{DS\,DS}s_j^{DS}$$
$$-\sum_{j=3,4,5}(A_{5j}^{DS\,FS_1}\ddot{s}_j^{FS_1} + B_{5j}^{DS\,FS_1}\dot{s}_j^{FS_1})$$
$$-\sum_{j=3,4,5}(A_{5j}^{DS\,FS_2}\ddot{s}_j^{FS_2} + B_{5j}^{DS\,FS_2}\dot{s}_j^{FS_2})$$
$$+ l_1 K_{air}^{DS\,FS_1}\left[s_3^{DS} - l_1 s_5^{DS} - s_3^{FS_1} + l_1 s_5^{FS_1}\right]$$
$$+ l_2 K_{air}^{DS\,FS_2}\left[s_3^{DS} - l_2 s_5^{DS} - s_3^{FS_2} + l_2 s_5^{FS_2}\right],$$

$$0 = F_3^{FS_1} - \sum_{j=3,4,5}(A_{3j}^{FS_1\,FS_1}\ddot{s}_j^{FS_1} + B_{3j}^{FS_1\,FS_1}\dot{s}_j^{FS_1})$$
$$-C_{33}^{FS_1\,FS_1}(s_3^{FS_1} - l_1 s_5^{FS_1}) - C_{34}^{FS_1\,FS_1}s_4^{FS_1} - C_{35}^{FS_1\,FS_1}s_5^{FS_1}$$
$$-\sum_{j=3,4,5}(A_{3j}^{FS_1\,FS_2}\ddot{s}_j^{FS_2} + B_{3j}^{FS_1\,FS_2}\dot{s}_j^{FS_2})$$
$$-\sum_{j=1}^{6}(A_{3j}^{FS_1\,DS}\ddot{s}_j^{DS} + B_{3j}^{FS_1\,DS}\dot{s}_j^{DS})$$
$$+ K_{air}^{FS_1}\left[s_3^{DS} - l_1 s_5^{DS} - s_3^{FS_1} + l_1 s_5^{FS_1}\right],$$

$$0 = F_5^{FS_1} - \sum_{j=1}^{6}(A_{5j}^{FS_1\,FS_1}\ddot{s}_j^{FS_1} + B_{5j}^{FS_1\,FS_1}\dot{s}_j^{FS_1})$$
$$-\sum_{j=3,4,5} C_{5j}^{FS_1\,FS_1}s_j^{FS_1} + l_1 C_{33}^{FS_1\,FS_1}(s_3^{FS_1} - l_1 s_5^{FS_1})$$
$$-\sum_{j=3,4,5}(A_{4j}^{FS_1\,FS_2}\ddot{s}_j^{FS_2} + B_{4j}^{FS_1\,FS_2}\dot{s}_j^{FS_2})$$
$$-\sum_{j=1}^{6}(A_{5j}^{FS_1\,DS}\ddot{s}_j^{DS} + B_{5j}^{FS_1\,DS}\dot{s}_j^{DS})$$
$$-l_1 K_{air}^{FS_1}\left[s_3^{DS} - l_1 s_5^{DS} - s_3^{FS_1} + l_1 s_5^{FS_1}\right],$$

$$0 = F_3^{FS_2} - \sum_{j=3,4,5}(A_{3j}^{FS_2\,FS_2}\ddot{s}_j^{FS_2} + B_{3j}^{FS_2\,FS_2}\dot{s}_j^{FS_2})$$
$$-C_{33}^{FS_2\,FS_2}(s_3^{FS_2} - l_2 s_5^{FS_2}) - C_{34}^{FS_2\,FS_2}s_4^{FS_2} - C_{35}^{FS_2\,FS_2}s_5^{FS_2}$$
$$-\sum_{j=3,4,5}(A_{3j}^{FS_2\,FS_1}\ddot{s}_j^{FS_1} + B_{3j}^{FS_2\,FS_1}\dot{s}_j^{FS_1})$$
$$-\sum_{j=1}^{6}(A_{3j}^{FS_2\,DS}\ddot{s}_j^{DS} + B_{3j}^{FS_2\,DS}\dot{s}_j^{DS})$$
$$+ K_{air}^{FS_2}\left[s_3^{DS} - l_2 s_5^{DS} - s_3^{FS_2} + l_2 s_5^{FS_2}\right] \text{ and}$$

$$
\begin{aligned}
0 = F_5^{FS_2} &- \sum_{j=1}^{6} (A_{5j}^{FS_2\,FS_2}\ddot{s}_j^{FS_2} + B_{5j}^{FS_2\,FS_2}\dot{s}_j^{FS_2}) \\
&- \sum_{j=3,4,5} C_{5j}^{FS_2\,FS_2} s_j^{FS_2} + l_2\, C_{33}^{FS_2\,FS_2}(s_3^{FS_2} - l_2\, s_5^{FS_2}) \\
&- \sum_{j=3,4,5} (A_{4j}^{FS_2\,FS_2}\ddot{s}_j^{FS_1} + B_{4j}^{FS_2\,FS_1}\dot{s}_j^{FS_1}) \\
&- \sum_{j=1}^{6} (A_{5j}^{FS_2\,DS}\ddot{s}_j^{DS} + B_{5j}^{FS_2\,DS}\dot{s}_j^{DS}) \\
&- l_2\; K_{air}^{FS_2}\left[s_3^{DS} - l_2 s_5^{DS} - s_3^{FS_2} + l_2 s_5^{FS_2} \right]. \qquad (20)
\end{aligned}
$$

Recognising that harmonic solutions are sought the velocities and accelerations are readily expressed in term of the unknown complex valued displacements. Expressing all other expressions in terms of their real and imaginary parts one may replace the complex equations of motion by twice the number of real equations and formulate them into a general real algebraic system for solution.

By combining the unmodified equations of Equations (11) with the modified equations of Equation (20) the resulting matrix system is expressible in the form $As = F$ with A define as in Equation (11d). The stiffness matrix in its most general form can be expressed as $C + K$ with C defined by Equations (11e) and the 'aerostatic' stiffness K defined according to the following set of definitions**:**

$$
[K] = \begin{bmatrix} K_{11} & K_{12} & K_{13} \\ K_{21} & K_{22} & K_{23} \\ K_{31} & K_{32} & K_{33} \end{bmatrix} \text{with the null sub-matrices}
$$

$$
[K_{23}] = \begin{bmatrix} 0 & 0 & 0 \\ 0 & 0 & 0 \\ 0 & 0 & 0 \end{bmatrix} = [K_{32}],
$$

and the remaining sub-matrices defined according to:

$$
[K_{11}] = \begin{bmatrix}
0 & 0 & 0 & 0 & 0 & 0 \\
0 & 0 & 0 & 0 & 0 & 0 \\
0 & 0 & K_{air}^{DS\,FS_1} + K_{air}^{DS\,FS_2} & 0 & -l_1 K_{air}^{DS\,FS_1} - l_2 K_{air}^{DS\,FS_2} & 0 \\
0 & 0 & 0 & 0 & 0 & 0 \\
0 & 0 & -l_1 K_{air}^{DS\,FS_1} - l_2 K_{air}^{DS\,FS_2} & 0 & l_1^2 K_{air}^{DS\,FS_1} + l_2^2 K_{air}^{DS\,FS_2} & 0 \\
0 & 0 & 0 & 0 & 0 & 0
\end{bmatrix},
$$

$$
[K_{12}] = \begin{bmatrix}
0 & 0 & 0 \\
0 & 0 & 0 \\
-K_{air}^{DS\,FS_1} & 0 & l_1 K_{air}^{DS\,FS_1} \\
0 & 0 & 0 \\
l_1 K_{air}^{DS\,FS_1} & 0 & -l_1^2 K_{air}^{DS\,FS_1} \\
0 & 0 & 0
\end{bmatrix},
$$

$$
[K_{13}] = \begin{bmatrix}
0 & 0 & 0 \\
0 & 0 & 0 \\
-K_{air}^{DS\,FS_2} & 0 & l_2 K_{air}^{DS\,FS_2} \\
0 & 0 & 0 \\
l_2 K_{air}^{DS\,FS_2} & 0 & -l_2^2 K_{air}^{DS\,FS_2} \\
0 & 0 & 0
\end{bmatrix},
$$

$$
[K_{22}] = \begin{bmatrix}
K_{air}^{FS_1} & 0 & -l_1\left(C_{33}^{FS_1} + K_{air}^{FS_1}\right) \\
0 & 0 & 0 \\
-l_1\left(C_{33}^{FS_1} + K_{air}^{FS_1}\right) & 0 & +l_1^2\left(C_{33}^{FS_1} + K_{air}^{FS_1}\right)
\end{bmatrix},
$$

$$
[K_{21}] = [K_{12}]_{air}^{T},
$$

$$
[K_{33}] = \begin{bmatrix}
K_{air}^{FS_2} & 0 & -l_2\left(C_{33}^{FS_2} + K_{air}^{FS_2}\right) \\
0 & 0 & 0 \\
-l_2\left(C_{33}^{FS_2} + K_{air}^{FS_2}\right) & 0 & +l_2^2\left(C_{33}^{FS_2} + K_{air}^{FS_2}\right)
\end{bmatrix}
$$

and $\quad [K_{31}] = [K_{13}]_{air}^{T} \qquad (21)$

Upon defining $[K_{12}]_{air} = [K_{12}]$ with $K_{air}^{DS\,FS_1}$ replaced by $K_{air}^{FS_1}$ and defining $[K_{13}]_{air} = [K_{13}]$ with $K_{air}^{DS\,FS_2}$ replaced by $K_{air}^{FS_2}$ completes specification of remaining submatrices defined in Equation (21). The individual stiffness terms involved are provided through the earlier presented definitions of Equation (19) with the specific heat ratio γ assigned a value of 1.4. For $\gamma = 1$ the integration implied at the beginning of Section 3.2 yields

$$
K_{air} = \frac{P_o A_o y_o}{y_{peak}^2}\left[\ln\left(1 - \frac{y_{peak}^2}{y_o^2}\right)\right]
$$

The only other additional modelling complexity considered is that of the viscous roll damping of the ship. Rather than deal with this in terms of direct calculation using discrete vortex models the following rather pragmatic model of modifying the inviscid pure roll fluid damping was applied for differing values of α, that is,

$$
\begin{aligned}
B_{44}^{DS\,DS} &\equiv \left[B_{44}^{inviscid} + \alpha\; B_{44}^{viscous}\left|\dot{s}_4\right| \right] \\
&= \left[B_{44}^{DS\,DS} + \alpha\,\omega . B_{44}^{viscous}\left|s_4\right| \right] \\
&\text{and} \qquad (22)
\end{aligned}
$$

$$
B_{44}^{viscous} = \underset{\omega \in [0,+\infty]}{Max}\left[B_{44}^{DS\,DS} \right]
$$

That is, $B_{44}^{viscous}$ is assigned the maximum value attained by $B_{44}^{DS\,DS}$.

Whilst known standard ranges of values for the radii of gyration associated with the pure roll, pitch and yaw

moments of inertia are readily available [Peach & Brook (1987)], there is no corresponding empirical means of estimating the values of the products of inertia.

The non-availability of the detailed mass distribution of the ship is the most likely reason why the products of inertia of an intact ship are nominally set to zero in most analyses. However, even if zero products of inertia are correct for the intact ship, it cannot be true for the damaged ship, due to the trim and heeling effects resulting from the damage and water ingress. Here it is sufficient to state that Hearn & Saydan (2004) have determined a novel method of estimating the products of inertia of a damaged ship assuming the intact ship values are zero. This method is used to provide the required values for the different damage scenarios of the Derbyshire provided in Table 2. The derivation of the associated logic and the sensitivity of the method are to be reported elsewhere.

Having provided the arguments for the theoretical extensions necessary to model responses of a damaged ship, sample motion response results are presented next for the intact and damaged form of the optimised Derbyshire hull.

5. PRESENTATION AND DISCUSSION OF RESULTS

Equations (10) were used by Saydan (2006) to determine motion responses for both the parent and optimised intact and damaged hull forms for regular harmonic progressing waves of unit amplitude (a=1.0m). The Matthew 3D diffraction suite was used to provide the hydrodynamic reactive and wave excitation loads together with the hydrostatic restoration terms for each distinct orientation of the hull corresponding to scenarios A to D of Tables 1 & 2.

As an initial simple cross check in this study the intact and damaged motion responses produced by Saydan (2006), using a Fortran program based on Equations (10), were readily reproduced using an Excel spreadsheet.

Here the MATTHEW diffraction suite (of Hearn) has been used to create the hydrodynamic and hydrostatic loads for the case of the damaged hull with one and two internal free surfaces, scenarios A & C respectively. Equality of the hydrodynamic reactive cross terms and the Haskind checks of wave excitation (Section 2.4) were found to be more than acceptable apart from a few sway-roll cross terms, as admitted at the end of Section 2.4.

The newly created hydrodynamic and hydrostatic data has then been used to generate the 'Simple' motion responses using Equations (11a) & (11b) for scenario A and all of Equations (11) for scenario C. The conditioning numbers (Section 2.5) associated with the hydrodynamic analysis and the motion responses were found to be more than satisfactory, indicating that all systems of linear equations were numerically stable.

Since the aerostatic stiffness of the internal air is a function of the motions of the ship and these motions also affect the mean level of the internal free surface (even though their position is assumed known a'priori in the hydrodynamic analysis) then the motion responses of the structure and the internal free surfaces must be determined iteratively. If the air stiffness influences are ignored initially then Equations (11) can be readily solved to provide a first estimate of the required motions. Next, from the estimated motion responses for the individual degrees of freedom of the ship (in particular the heave, roll and pitch motions) one may determine the RVM of the hold at a point vertically above the free surface centroid (see Figure 4). The mean air gap between selected free surface and deck y_0 (typically of the order of 8m) is known for each scenario and so the new mean position of the internal free surface y_1 can be determined from solving the transcendental form of Equation (16) or using a tabulated form of Figure 5 with interpolation. The latter method was used to speed up the calculations. Knowing the resultant vertical motion of the free surface at its centroid, from the motion responses of the internal free surface, means that $y_{peak}^{FS_i}$ can be determined for the appropriate free surfaces in existence. Hence Equations (19) may now be used to determine the various aerostatic stiffness terms required to generalise Equations (11) to reflect the needs of Equations (20) and (21). Next the motion equations can be resolved and the whole process applied iteratively until convergence of all responses is achieved. This procedure was generated in an Excel spreadsheet using Visual Basic based macros, rather than writing a Fortran computer program. The responses predicted with inclusion of air stiffness influences are designated 'Full Stiffness Model'.

For additional curiosity the roll damping of the ship was nonlinearised in accordance with Equation (22). Hence the iteration of the roll response, if significant, would also impact on the iterations of the air stiffness matrix and the resulting transfer functions. When results include additional 'viscous' roll damping as well as the complete air stiffness effect the designation is 'Full Stiffness Model B0'

As results presented will indicate the inclusion of the non-linear roll damping was less significant that the inclusion of the aerostatic stiffness.

A complete presentation of all the computed motions for each substructure for a wide range of wave headings would require presentation of an excessive number of figures. Interested parties can request copies of such details provided in an internal Ship Science report. Here results are restricted to essentially a wave heading of 135^o (equally described as a heading of 45^o onto the starboard bow). However, because of the heel and trim

of the damaged ship the roll and pitch responses change if the wave heading is changed from 45° on the starboard bow to 45° on the port bow (corresponding to a heading of 225°). The corresponding heave motions are much less sensitive. In all the calculations presented $\gamma = 1.4$, although the influence of the gamma value is not significant (as illustrated in Figure 5).

The impact of the number of free surfaces present upon the heave, roll and pitch as a function of the state of the hull (intact or damaged) and the analysis method used is provided in Figures 7(a) & (b), 8(a) & (b) and 9(a) & (b) respectively. These figures indicate that the impact of including the aerostatic stiffness is significant upon the ship transfer functions.

The vector sum of these motions at any selected point provides an estimate of the relative vertical motion (RVM) at a selected point. In Saydan (2006) the RVM was calculated at 8 distinct points (using Equations (10) only) and this demonstrated how the damaged state of the ship could change as one moved from between bow, amidships and stern and port & starboard. Here we shall consider the point corresponding to the bow of the intact ship (designated point A) and the amidships point on the port side (designated point C). Figures 10 (a) & (b) and Figures 10 (c) & (d) indicate how RVM changes with the particular damage scenario (case) as the point selected moves from the original bow to the deck amidships position respectively. The influence of the wave approach changing from starboard to port is provided upon comparing Figures 10 (c) & (d) with Figures 10 (e) & (f). The large motions of the internal free surface cited earlier, as a consequence of not including air stiffness influences for scenario A for the original wave heading is illustrated in Figure 11(a). Modelling only heave and not including roll and pitch degrees of freedom in the modelling of the free surface provides very excessive unrealistic motions. For further comparison Figures 11(b) & (c) provide the motions of both internal free surfaces for scenario C.

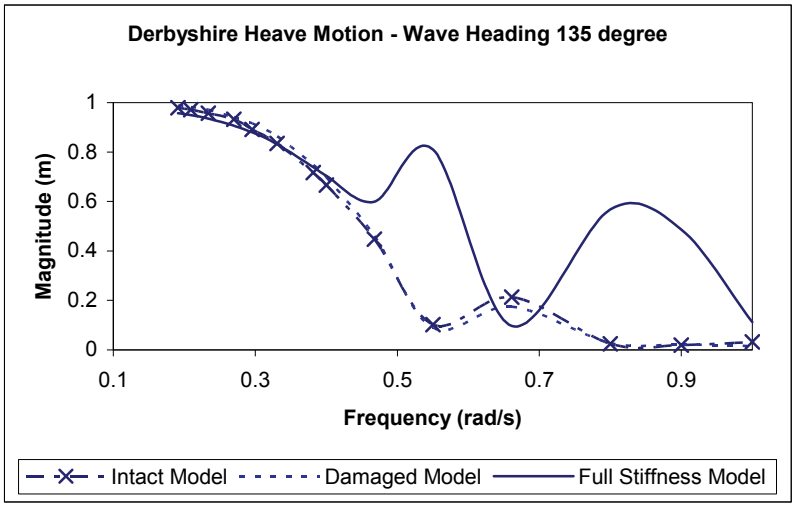

Figure 7(a) – Heave response for Case A at point corresponding to bow of intact hull form for a=1.0m

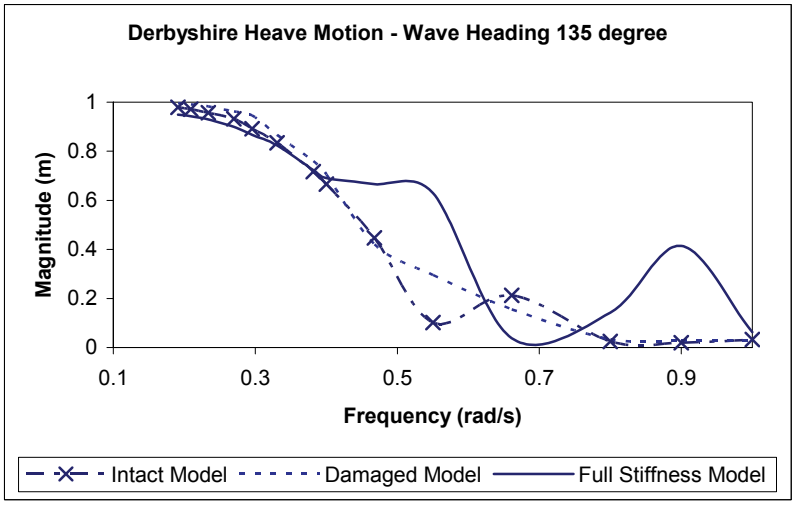

Figure 7(b) – Heave response for Case C at point corresponding to bow of intact hull form for a=1.0m

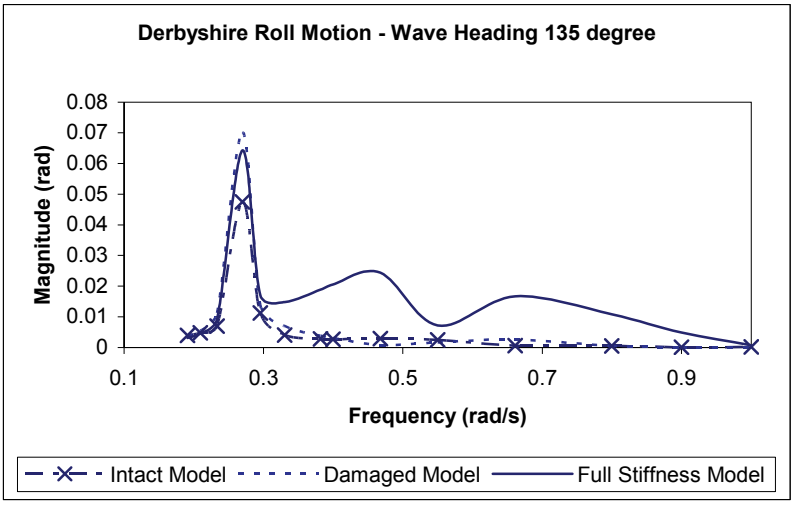

Figure 8(a) – Roll response for Case A at point corresponding to bow of intact hull form for a=1.0m.

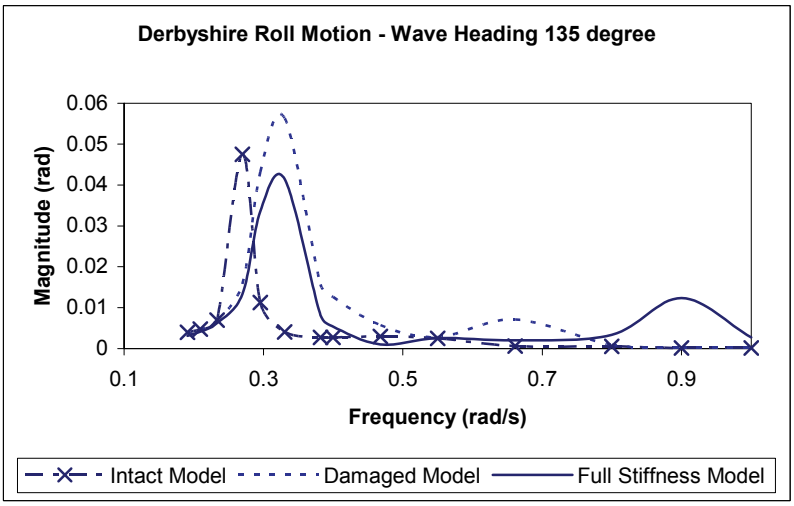

Figure 8(b) – Roll response for Case C at point corresponding to bow of intact hull form for a=1.0m.

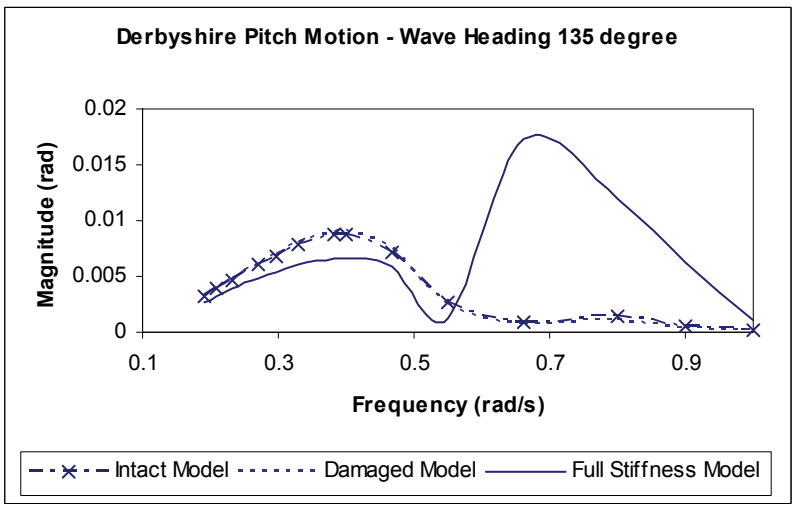

Figure 9(a) – Pitch response for Case A at point corresponding to bow of intact hull form for a=1.0m

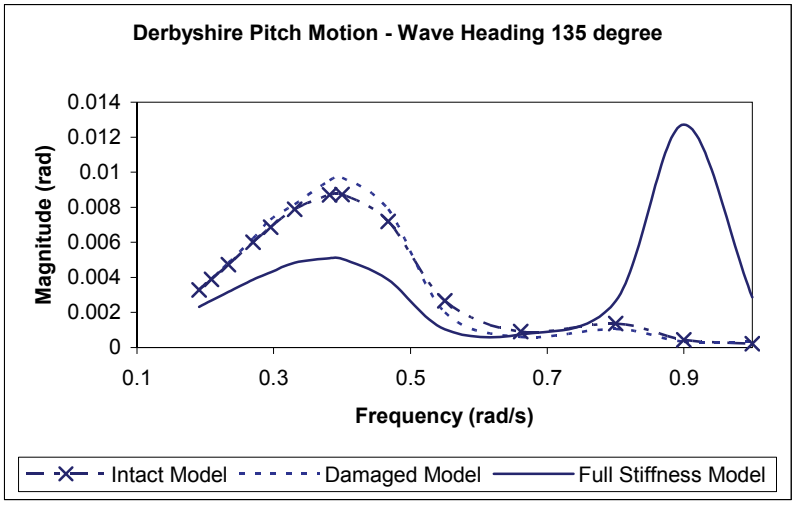

Figure 9(b) – Pitch response for Case C at point corresponding to bow of intact hull form for a=1.0m

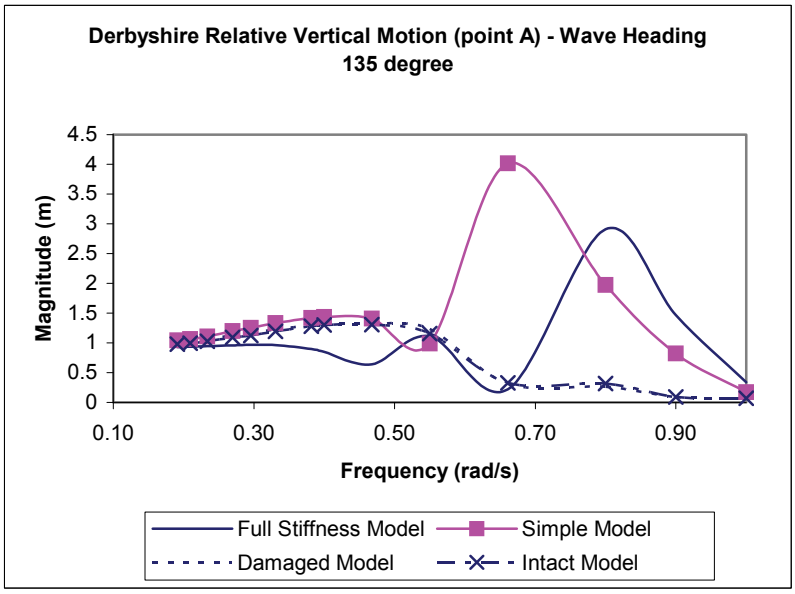

Figure 10(a) – Vertical relative motion response for Case A at point corresponding to bow of intact hull form for a=1.0m

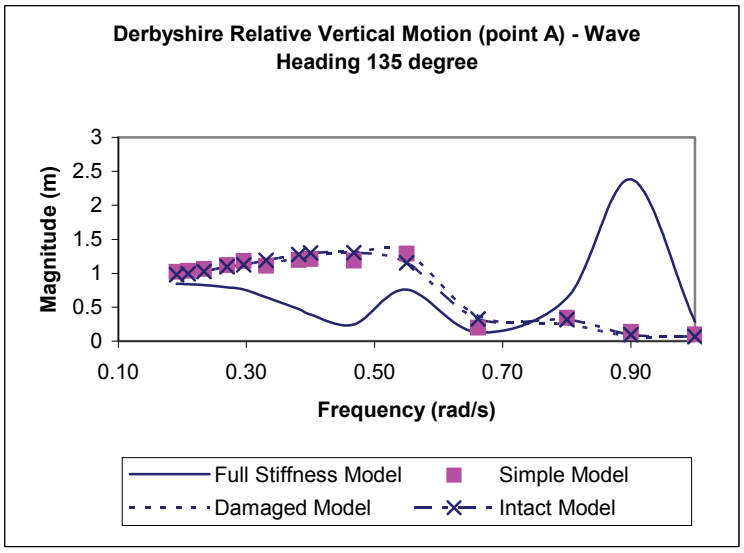

Figure 10(b) – Vertical relative motion response for Case C at point corresponding to bow of intact hull form for a=1.0m

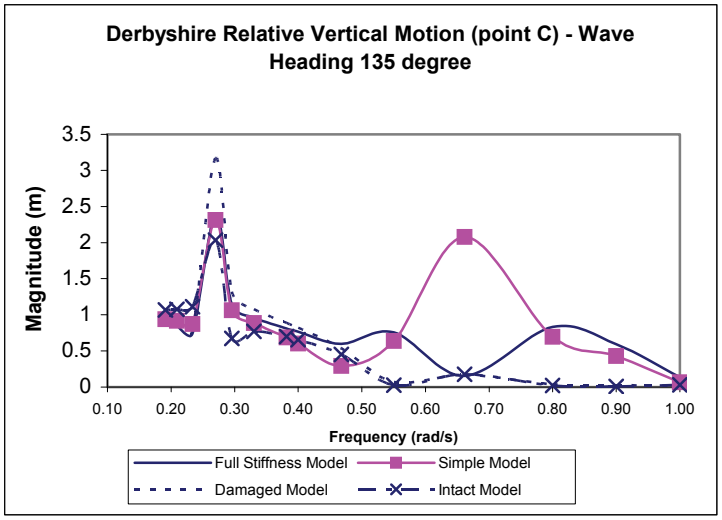

Figure 10(c) – Vertical relative motion response for Case A at point corresponding to amidships point on deck on port side for a=1.0m.

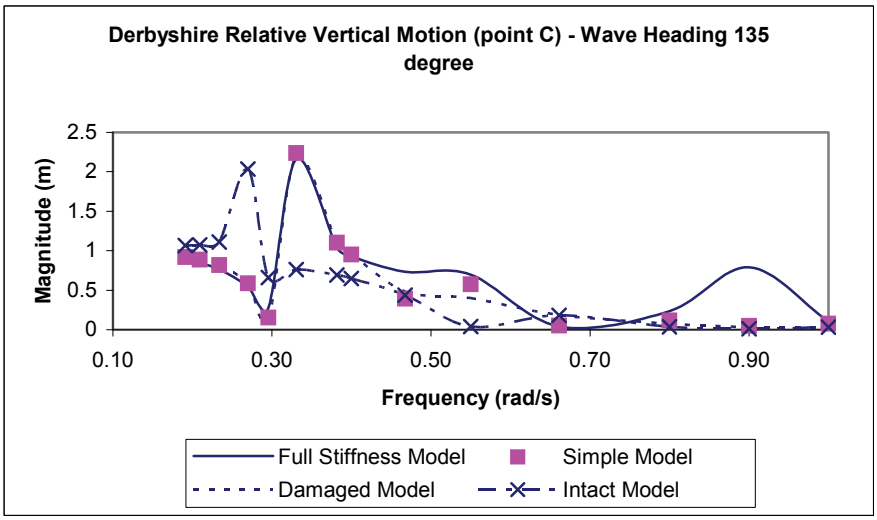

Figure 10(d) – Vertical relative motion response for Case C at point corresponding to amidships point on deck on port side for a=1.0m

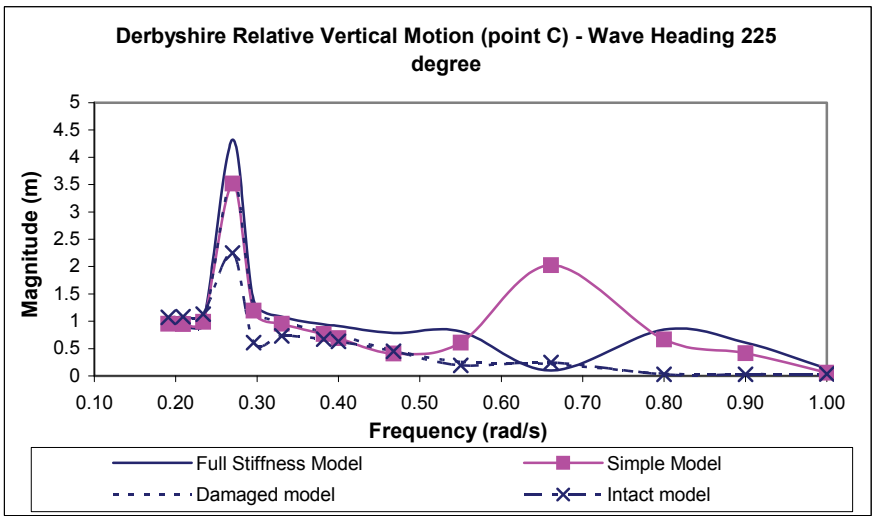

Figure 10(e) – Vertical relative motion response for Case A at point corresponding to amidships point on deck on port side for a=1.0m

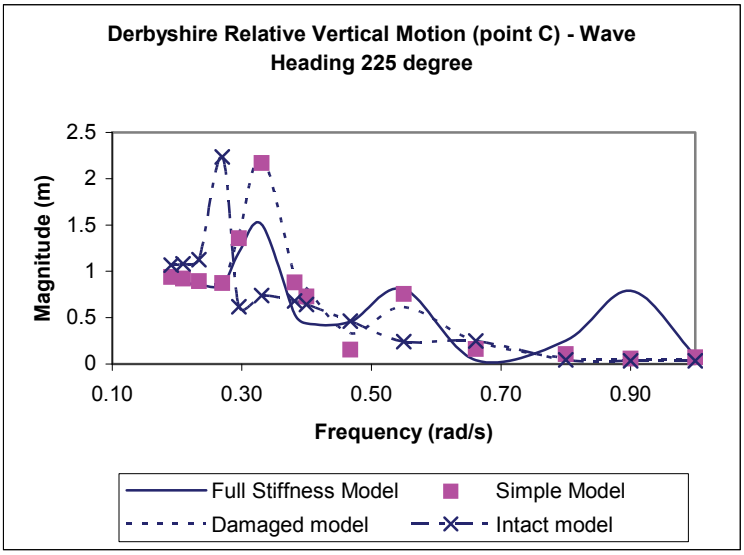

Figure 10(f) – Vertical relative motion response for Case C at point corresponding to amidships point on deck on port side for a=1.0m

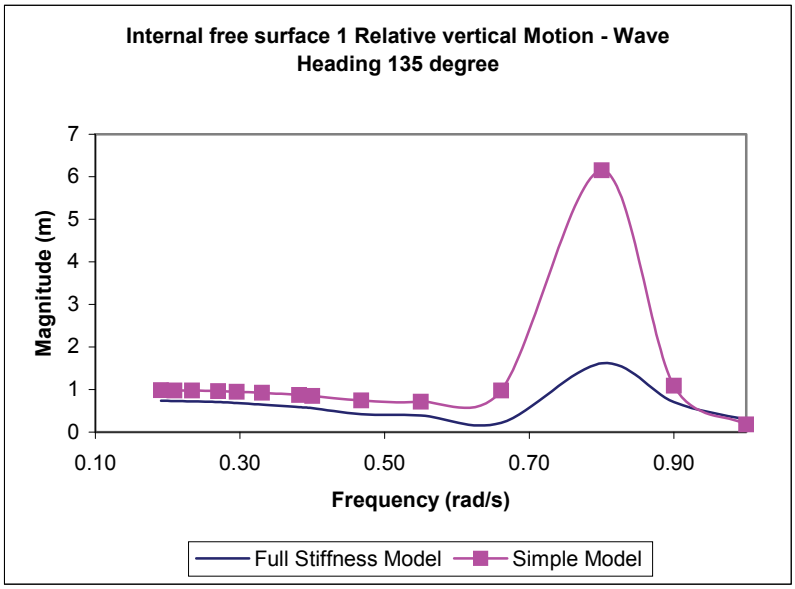

Figure 11(a) – Vertical relative motion response for Case A at centroid of free surface for a=1.0m

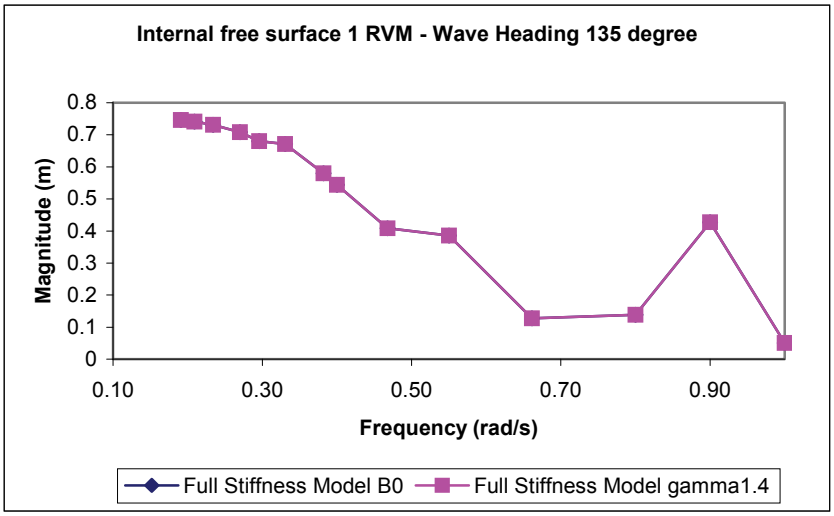

Figure 11(b) – Vertical relative motion response for Case C at centroid of free surface for a=1.0m

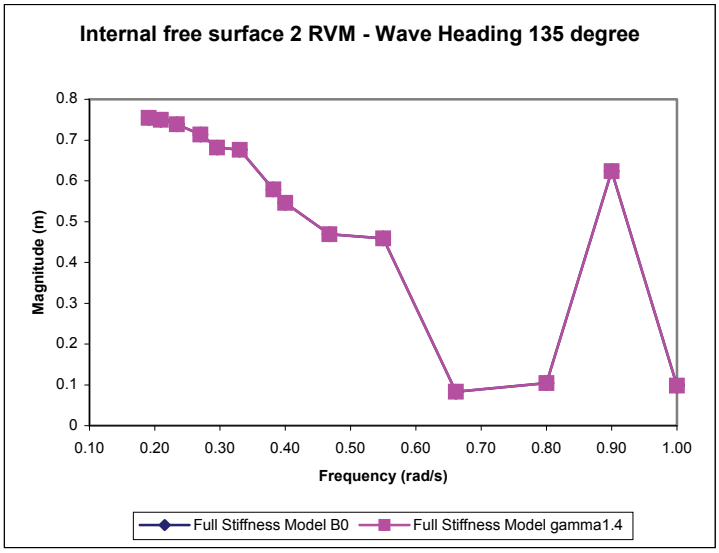

Figure 11(c) – Vertical relative motion response for Case C at centroid of free surface for a=1.0m

6. CONCLUSIONS AND CLOSING COMMENTS

This paper has presented a novel extension of the motion response equations to include the hydrodynamic and hydrostatic influences of the internal free surfaces and the aerostatic influences of the air contained within the damaged hold above the internal free surfaces. The inclusion of the change of the mean position of the internal free surface as a consequence of the relative phasing of the motions of the ship and the internal free surfaces is also new. Typically the calculated value of y_1 was found to vary between 0.35m and 0.5m depending upon the wave direction and frequency. This range includes differences between the two free surfaces of scenario C. The ability of the MATTHEW diffraction suite to cope with internal free surfaces was an original existing feature.

The results presented here indicate that the motions of the damaged ship are greater using the new proposed modelling than those derived for the damaged ship using the more conventional formulation of Equations (10). Folsø et al (2007) carried out a similar study for a double hull tanker using standard formulations of the hydrodynamic and motion response formulations. Again different degrees of damage with corresponding details similar to Tables 1 & 2 were presented. Again zero speed Green functions were used for the hydrodynamic analysis. In this case forward speed corrections were applied and the influence of the motion changes upon horizontal and vertical bending moments. Other papers addressing flooding and damaged ships are addressed in these proceedings.

The possibility of 3 holds being damaged for this ship type is unlikely, but having considered one and then two possible internal free surfaces in some detail in this paper, the methodologies presented can be readily generalised to more internal free surfaces if the need arose. In fact one might suggest partitioning the free surfaces into a number of subordinate mass-less plates to increase the complexity of the modelling and to ascertain whether the assumption of the free surface moving as a single flat surface is reasonable.

The proposed analysis method has been applied to an oscillating water column wave energy extraction device modelled as a bottom standing and floating structure with internal free surface modelled as a mass less plate.

7. ACKNOWLEDGEMENTS

The principal author is pleased to acknowledge the contribution of M. Lafforgue and M. Perdriset whilst completing the final year project of their French degree at the University of Southampton. They were both a delight to work with and were extremely industrious over their 4-month visit. Dr. Mingyi Tan is thanked for assistance with Figures 2 & 6.

8. REFERENCES

1. Day, A.H. and Doctors, L.J. (1997) Design of fast ships for minimal resistance and motions. Proceedings of 5th International Marine Design Conference, IMDC'97, University of Newcastle upon Tyne, pp. 569-583.

2. Doctors, L.J. and Day, A.H. (1995) Hydrodynamically optimal hull forms for river ferries. Proceedings of RINA International Symposium on High Speed Vessels for Transport and Design, RINA, London, Paper No. 5 pp.1-21

3. Faltinsen, O. and Michelsen, F. C. (1974) Motions of Large structures at Zero Froude Number. Proceedings of International Symposium on the Dynamics of Marine Vehicles & Structures in Waves, London, Paper 11, pp. 99 – 114.

4. Folsø, L., Rizzuto, E and Pino, E. (2007) Wave induced global loads for a damaged vessel. Proceedings of Advancements in Marine Structures, Edited by Guedes Soares and Purnendo Das, Glasgow, Published by Taylor & Francis, pp. 11-22.

5. Gow, Margaret M. (1964) A Course in Pure Mathematics. First Edition 4th Impression The English Universities Press Ltd. 1964 (See in particular Section 4.15 pp. 62-63)

6. Gradshetyn, I.S. and Ryzhik, I.M. (1965) Tables of integration, Series and Products. Translated from Russian by Scripta Technica Inc and Translation Edited by Alan Jeffrey Academic Press 4th Edition 1965.

7. Haskind, M.D (1954). Approximate Methods of Determination of Hydrodynamic Characteristics of Ship Oscillations. Investiya Akad. Naut. SSSR. Okd, Tech, Naut., No 11, p. 66 (In Russian).

8. Hearn G. E., Hills W. & Sarıoz K. (1992). *Practical Seakeeping for Design: A Ship Shape Approach* Presented as Paper No.2, RINA Spring Meeting, April 1991 and RINA Trans. Vol. 134, pp. 225-244.

9. Hearn G. E., Hills W. & Yaakob O. B. (1995a) *Computer Aided Design of Fishing Boats for Improved Seakeeping Performance.* Proceedings of RINA International Conference on Computer Aided Design & Production for Small Craft, CADAP'95. Paper 18, 13pp.

10. Hearn, G.E., Wright, P.N.H. and Yaakob, O (1995b) Seakeeping for design: Identification of hydrodynamically optimal hull forms for large high-speed catamarans. Proceedings of RINA International Symposium on High Speed Vessels for Transport ands Defence, London, UK, Paper No. 4, pp. 1-15

11. Hearn G. E. (1977) *Alternative Methods of Evaluation of Green's Function in Three - Dimensional Ship-Wave Problems*. Journal of Ship Research, Vol.21, No.2, pp. 89-93.

12. Hearn. G. E. and Wright P.N.H. (1998). Optimal hull form design for seakeeping and resistance: a genetic algorithm based inverse method. In Proceedings of Third Osaka Colloquium on Advanced CFD Applications in Ship Flow and Hull Form Design, OC'98, Osaka, Japan, pp.499-514.

13. Hearn, G.E. and Wright, P.N.H. (1999). Design for optimal hydrodynamic operation of large container ship. Proceedings of the RINA International Conference on Design and Operation of Container Ships, London, UK, Paper No. 5, pp.1-13.

14. Hogben, N and Standing, R.G. (1974). Wave loads on Large Bodies. Proceedings of International Symposium on the Dynamics of Marine Vehicles & Structures in Waves, UCL, London, Paper 26, pp. 273 – 292.

15. Hooke, R and Jeeves, T.A. (1961), "Direct search" solution of numerical and statistical problems, Journal of the Association for Computing Machinery, Vol. 8, pp. 212-229.

16. Newman, J. N. (1965) The Exciting Forces on Moving Body in Waves. Journal of Ship Research, Vol. 9, pp. 190 – 199.

17. Odabasi, Y. and Hearn, G.E. (1977) Seakeeping Theories: What is the Choice? Transactions of NECIES, Vol. 94, No. 3, pp. 53-84.

18. Peach, R.W. and Brook, K. (1987) The radii of gyration of merchant ships. Transactions of NECIES, Vol. 103, No. 3, pp.115 –117.

19. Sarıoz K., Hearn G. E. and Hills W. (1992). Practical Seakeeping for Design: An Optimised Approach. Proceedings of PRADS, University of Newcastle, Vol. 1., pp. 1.233 – 1. 245.

20. Sarıoz, K (1997) A Hydrodynamic Hull Form Design Procedure in Conceptual and Preliminary Ship Design. PhD Thesis, The University of Newcastle upon Tyne, UK.

21. Saydan, D. and Hearn, G.E. (2004) Damage stability as a safety criterion for optimisation tools. Proceedings of 4th International Conference on High Performance Marine Vehicles, Rome, Italy, pp. 177-191.

22. Saydan, D (2006). Damage Stability of Ships as a Safety Criterion for Optimisation Tools. PhD Thesis, The University of Southampton, UK.

23. Wilson, P.A. (1986) A Seakeeping analysis of a family of merchant ships. Proceedings of International Conference on Computer Aided Design, Manufacture and Optimisation in the Marine and Offshore Industry, Washington DC, USA, pp. 237-253

24. Wright, P.N.H. (2004) The Preliminary Design of Catamarans for Seakeeping and Resistance, PhD Thesis, The University of Newcastle upon Tyne, UK.